UNIVERSITY of CALIFORNIA

SANTA CRUZ

INTERSTRIP CHARACTERIZATION OF SILICON STRIP DETECTORS

A thesis submitted in partial satisfaction of the
requirements for the degree of

BACHELOR OF SCIENCE

in

PHYSICS

by

Sara Lindgren

11 June 2009

The thesis of Sara Lindgren is approved by:

Professor Hartmut F. -W. Sadrozinski Technical Advisor	Professor David P. Belanger Thesis Advisor

Professor David P. Belanger
Chair, Department of Physics

Abstract

The interstrip characteristics of silicon strip detectors are important for the proper functionality of the detector. The radiation hardness of these devices is crucial since they will be exposed to high levels of radiation when used. With the high luminosity upgrade for the Large Hadron Collider at CERN the ATLAS detectors will be exposed to fluences of up to 10^{16} neq/cm^2. In the aim to design the most radiation tolerant detectors several different strip isolation structures have been tested, i.e. by applying different doses of p-spray and p-stops. The interstrip resistance and capacitance are measured by using the concept of two neighbors- and one test strip. The detectors tested are P-type silicon strip detectors from the 2^{nd} and 3^{rd} prototyping runs with Hamamatsu Photonics for the ATLAS upgrade program. The measurements were done before and after controlled irradiation with 70 MeV protons to a fluence of $1.5 \cdot 10^{13}$ p/cm^2 and $1.14 \cdot 10^{13}$ p/cm^2, corresponding to about 1 MRad.

Contents

List of Figures

Acknowledgements

I first want to thank my family and friends who always has been a great inspiration for me and especially Davide for his love and support both in good and bad moments throughout the process of completing this thesis. I also owe a great thank to Noel Mayur Dawson, Christopher Betancourt, Gatlin Bredeson and all the other students in the SCIPP laboratory for taking their time and effort to teach me the methods and theories for the different experiments I have been a part of during this year. I also will take the opportunity to here point out that some of the data for which the thesis is funded upon is taken in collaboration with Noel Mayur Dawson and Gatlin Bredeson for which help I am very grateful.

Last I am enormous grateful that Professor Hartmut F.-W. Sadrozinski who gave me the opportunity to work at the SCIPP laboratory and write my thesis upon my research. I want to thank him for his supports and encouragement in everything which made me feel welcome and inspired. I am also grateful for that he always has been pushing me to take on new challenger and projects. This has given me great experience and knowledge, not only in the contents of my thesis but also in many neighboring fields. Last I want to dedicate this thesis to my father, Carl-Henrik Lindgren, the reason I am studying and love physics.

1

Introduction

1.1 Silicon Strip Detector

In the search for the heavier quarks, strange and charm, in the 1970 scientists needed new types of detectors and detector material since the devices of that time were not accurate enough. In today's high-energy physics it is required that detectors can determine the position of particles with very high accuracy and with short response time since many of the particles in question will decay within a fraction of a second and therefore only travel a short distance. The first step to today's detectors was taken with the success of developing single-crystal silicon. The next step was the silicon strip detectors (SSD) which have silicon's fast response and the strips provide a high spatial resolution to the detector. [1] Silicon strip detectors are P-N junctions and are essentially complicated diodes. In a diode the junction is planar while in a SSD heavily doped strips are implanted on top of an oppositely doped bulk. [2]

If we look closer on some of the important structures in a SSD the outermost one are the guard rings, only one for the Hamamatsu detectors. Whose purpose is to reduce the risk of electrical breakdown by lowering the voltage which is applied to the backplane so the voltage that reaching the bias ring is at ground potential. Inside the guard rings is the bias ring and inside it the strips. Each strip has AC- and DC- pads to which one can connect for testing and on one side the strips are connected to the bias ring through resistors. Silicon strip detectors are functioning under reverse bias where the voltage is applied to the backplane and the bias ring is grounded.

1.2 P-type detector

There are two types of SSDs, so called P- and N-type. The P-type SSDs, also called n-on-p sensor, are built up of a lightly p-doped silicon bulk with heavily n-doped strips implanted on the top and highly p-doped material on the bottom. The top surface is covered by silicon oxide and the bottom with an aluminum layer. Each strip is then covered by a thin layer of aluminum, see fig. 1.1. The silicon oxide layer is applied to give a capacitor between the strip itself and the aluminum on top of them so the read-out equipment will give an AC-signal. The oxide layer will also provide a faster read-out and reduce the noise.

Today the P-type detectors are believed to have some advances compared to N-type detectors. They can operate under-depleted after high fluences, they typically have a longer lifetime and type inversion during high radiation is unlikely.

Also the mobility of electrons is greater compared to the hole mobility which will allow them to have shorter response time and finally they are expected to be cheaper than n-on-n sensor because they require only single-sided processing. [3] One disadvantage is that the surface of the P-type detectors might be more sensitive to radiation.

When a charge particle enters the detector it will ionize silicon atoms in its path through the bulk and electron-hole pairs are produced, so called charge carrier. The electro-static charge from the construction of the detector will make the charge carrier to travel against an opposite charge; the holes drift to the backplane and the electrons to the strips. The signal is read out by the electronics applied to the conductive aluminum layer on the strips.

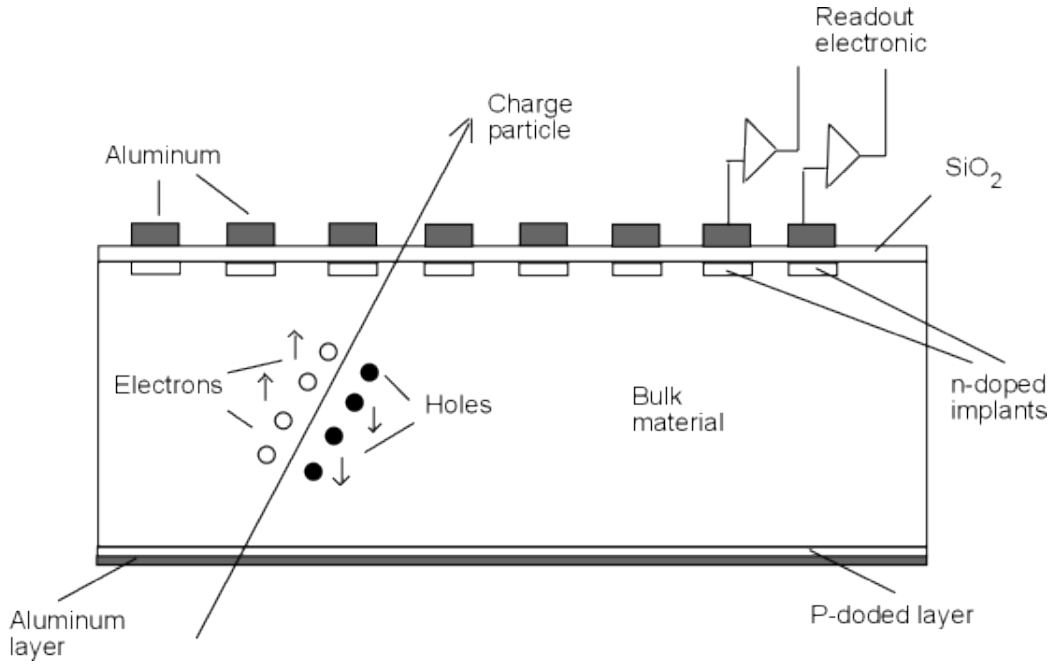

Figure 1.1: *A sketch of a P-type silicon strip detector. The detectors' structure is a bulk of lightly p-doped silicon with highly n-doped strips implanted on the surface and a highly p-doped layer on the bottom. Both the bottom layer and the strips are covered by a thin layer of conducting aluminum. When a charge particle enters the silicon bulk it will ionize the silicon atoms in its path and electron-hole pairs are produced, so called charge carrier. Due to the electro-static charge from the construction of the detector the charge carrier will travel against an opposite charge; the holes drift to the backplane and the electrons to the strips. The signal will then be read out by the electronics applied to the aluminum layer on the strips.*

1.3 Radiation damage

Today SSDs are used in many experiments around the world there the ATLAS detector at the Large Hadron Collider (LHC) at CERN will employ many of these SSDs in its inner detector. The problem for most detectors is since they are operating close to the actual collision point the silicon devices, electronics and all other mechanical equipment are exposed to enormous amounts of radiation. To know that the detector will operate properly during a long runtime they need to be radiation hard.

The plans for an upgrade of the luminosity, to approximately $10^{35}\ cm^{-2}s^{-1}$, at the LHC will require a need for a great increase in radiation hardness especially for the multipurpose detectors, ATLAS and CMS. To be able to use the whole physical potential for such an upgrade, some of the detectors will be exposed to a hadron fluence as high as $10^{16}\ cm^{-2}$ during a five years period. For investigation in this manner a project within CERN was created called RD-50 "Development of Radiation Hard Semiconductor Devices for Very High Luminosity Collider". [4]

There are different types of radiation damage; bulk and surface. Depending on how energetic and especially which type of particle the radiation is, the damage will differ. Two of the most common damaging radiation particles are proton and neutrons. Protons will ionize the atoms in its path through the detector which is mostly damaging to the surface. The neutrons will instead give a non-ionizing energy loss which might displaces silicon atoms from the bulk and give rise to severe bulk damage.

At heavy neutron radiation even so called type inversion can occur, i.e. for N-type detectors the bulk material will change from n-doped to p-doped. [5] In this thesis I will not take into account the above mentioned differences since all analyzed detectors have been exposed to the same radiation particles with the same particle energy. All fluences are approximately the same.

1.4 Structures

As earlier mention P-type detectors are thought to have a more sensitive surface than p-on-n sensor. A specific concern is the risk that the fixed oxide charges in the Si-SiO_2 interface would lead to a conductive layer of electrons. [6] Within the project ATLAS07 for the ATLAS upgrade different structures for mini-SSDs, the so called pre-series, have been produced. The different structures use the concept of preventing those damages by surface treatments like positive doped implants (p-impurities) in form of p-stop or p-spray, or a combination of both.

The p-stops are implanted to the detectors with a mask while p-spray is sprayed on. The dose and which positive impurity, p-stops or p-spray, a specific detector has been treated with are indicated by its wafer number. Different structures, the mask, to apply the p-stops have also been used. This is indicated by the detectors different zones. The data analyzed in this thesis is from the 2^{nd} and 3^{rd} pre-series, hence I will focus on the structures within those two generations.

For the 2^{nd} pre-series the different detectors available at SCIPP has wafer 1, 25, 31 and 35. Wafer 1 has both p-spray and p-stops, both to a dose of $2 \cdot 10^{12}$ cm^{-2}, give a total dose of $4 \cdot 10^{12}$ cm^{-2}. Detectors with wafer 25 only have p-stops to a dose of $2 \cdot 10^{12}$ cm^{-2} and detectors with wafer 31 have p-stops but with a higher dose of $4 \cdot 10^{12}$ cm^{-2}. Finally there are detectors with wafer 35 which have p-spray, i.e. the mask for the p-stops was left out. The dose of p-spray is $2 \cdot 10^{12}$ cm^{-2}, see table 1.1. Regarding the doses of the 2^{nd} series the manufacturers can not ensure that all the doses are exactly as stated above.

Table 1.1: *Doses of p-impurities for the 2^{nd} series*

Wafer number	1	25	31	25
p-spray	$2 \cdot 10^{12}$	-	-	$2 \cdot 10^{12}$
p-stop	$2 \cdot 10^{12}$	$2 \cdot 10^{12}$	$4 \cdot 10^{12}$	-

The 3^{rd} pre-series consists of detectors with wafer 02, 12, 23, 33, 40, 42, 44 and 46 which correspond to identification letters A trough H. The different eight identification numbers have different doses of p-spray and p-stops, see table 1.2

Table 1.2: *Doses of p-impurities for the 3^{rd} series*

ID	A	B	C	D	E	F	G	H
Wafer number	02	12	23	33	40	42	44	46
p-spray	$2 \cdot 10^{12}$	-	-	-	$1 \cdot 10^{12}$	$2 \cdot 10^{12}$	$4 \cdot 10^{12}$	$2 \cdot 10^{12}$
p-stop	$2 \cdot 10^{12}$	$1 \cdot 10^{12}$	$2 \cdot 10^{12}$	$4 \cdot 10^{12}$	-	-	-	$8 \cdot 10^{12}$

For both the 2^{nd} and 3^{rd} series different zones are used, namely six different. The differences between those zones are variations in punch-through protection, the width of the conductive aluminum layer on each strip and the width of the pitch.

No figure with the structures can be shown due to an agreement with the manufactory since the detectors are still under prototyping. Detector with zone 1 which has no structure, i.e. they have only p-spray since the p-stop mask was left out. Detectors with zone 2 which has individual p-stops, i.e. each strip is surrounded by p-implants in opposite to the other structures which only have a line of p- implants between the strips. Zones 3 share the p-stops between the strips and zones 4 have added punch-through structure, this will be more discussed in next section. Detectors with zone 5 have narrow metal which means the aluminum layer over the strips do not reach outside the strip itself and finally zone 6 which have wider than for the remaining zones. [7]

Within the 3^{rd} series there are also different versions of the detectors with zone 4, regarding the punch-through protection. The difference between these is the geometry of the p-stops in the punch-through structure. Zone 4-A and 4-B have the same structure, only the arrangement differs. Zone 4-C has less implants and finally zone 4-D has the least implants, only around the entire structure. When referring to those detectors later in this thesis the ones with zone 4-A will also be indicated by P4, zone 4-B as P10, zone 4-C as P16 and finally 4-D as P22. Important is that those structure were never meant to be used with p-spray so one have to be observant with detectors with zone 4 and wafer 02, 40, 42, 44 and 46. [8]

1.5 Interstrip Resistance, Capacitance and Breakdown Voltage

Two important properties for a properly functioning SSD are the interstrip resistance and capacitance. If the resistance between the strips is too low a signal can transfer between the different strips and a hit will be counted in multiplied channels. There are two minimum values for the resistance which are important in the analysis for the ATLAS upgrade. Since the detectors tested for this thesis are part of the pre-series they are smaller than the ones which will be used in the ATLAS detector.

The SSDs tested have strips which are about 1 cm while they in full-sized will be about 10 cm. This is needed to take into account since the interstrip resistance depends on the length of the strip. For detectors analyzed in this thesis the resistance needs to be over 10^7 ohms while with the 10 cm detectors used in ATLAS the resistance needs to be over 10^8 ohms. Both those values are set so no signals will be transferred between the strips.

Another important function is the capacitance between the different strips and with in the strip itself. The noise for a detector is determined by

$$A + B \cdot C \tag{1.1}$$

there A and B is constants mostly based on the construction of the front-end chip which do not change with radiation. So the only factor that will change during radiation is C, the interstrip capacitance.

This means that the interstrip capacitance needs to be low in order to have a high signal to noise ratio. [9] Besides the damage radiation can cause to the interstrip properties it might lead to a magnified leakage current. The leakage current is the current all semiconductors have when operated under reversed bias. At one point the leakage current will start grow exponential and the detector does not function properly beyond this point. This is the so called breakdown voltage and this voltage might be affected by radiation.

2

Experiment

The data for this thesis is based on mini-SSDs with test structure produced by Hamamatsu Photonic (HPK) within the ATLAS upgrade program. The analysis is based on data taken before and after irradiation with 70MeV protons at a fluence of $1.5 \cdot 10^{13}$ p/cm^2 for the 2^{nd} series and $1.14 \cdot 10^{13}$ p/cm^2 for the 3^{rd}, both corresponding to about 1 MRad in total dose. The irradiation was done at CYRIC, Tohoku University, Japan.

The proton irradiation are done at a relative low fluence which is preferable for studies of the interstrip resistance and capacitance since they then can be studied independent of large bulk current, i.e. without cooling. Those measurements will be valuable even if the actual radiation for an ATLAS detector is going to be up to 10^3 times higher. This is because the radiation damage affecting the interstrip capacitance and resistance is mostly due to surface damage which will saturated after a relative low irradiation fluence.

2.1 R_{int} Measurement

To measure the interstrip resistance a probe station was used to connect to the DC pads of the strips. One strip is used as a test strip and the closest strips on each side as neighbor strips as seen in fig. 2.1. The test current will be refered as I_1, the neighbor current as I_2 and the neighbor voltage as V_2. The purpose of this setup is to measure the current in the test strip due to the applied voltage on the neighbors and from this calculate the interstrip resistance.

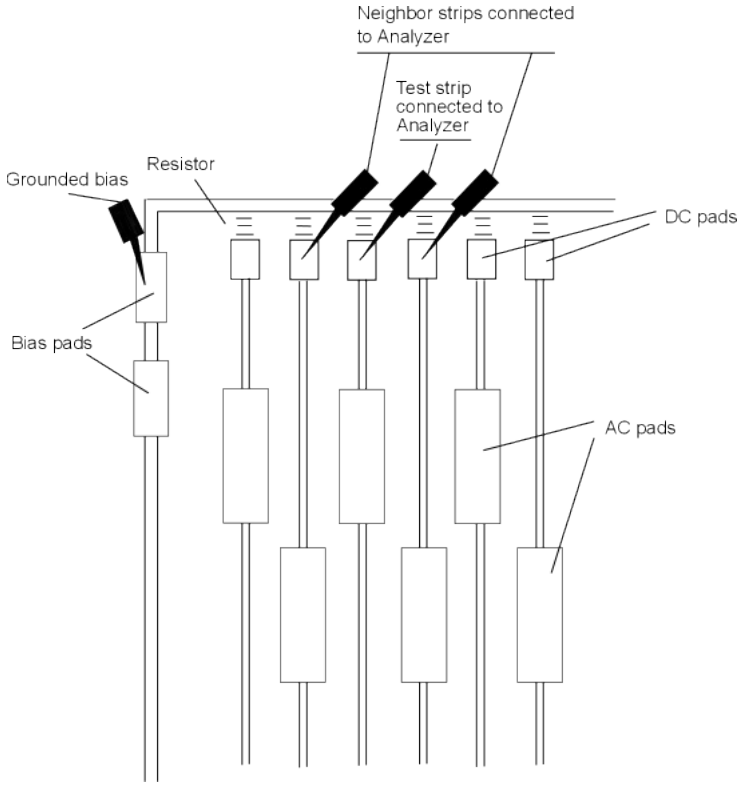

Figure 2.1: *The concept used for testing the interstrip resistance. Probes are touched down on the DC pads of the neighbors- and test strip. A probe is also touched down at a bias pad. The probes are when trough wires connected to the different electronics with which help the measurement is done.*

Two different methods have been used throughout this experiment but the different methods do not make any different in the accuracy of the data. The difference is only how the parameter analyzer was used. For both methods the probes from the neighbor strips are commonly connected to a parameter analyzer to which the test strip also is connected. The bias ring is connected to ground and a bias voltage varying between -5, -20, -50, -100 and -300 volts is applied to the backplane.

The difference between the methods is that for one method the voltage applied to the neighbor strips was manually changed between -1 and 1 volt, with steps of ± 1, ± 0.5 ± 0.2 and 0 while in the second method this is done by the sweep function of the analyzer which also varies the input from 1 volt but in steps of 100mV. All measurements were done at room temperature with nitrogen gas flowing over the detector.

Since the measured current will vary one used a generalized version of ohms law to determine the interstrip resistance.

$$R_{int} = \frac{2}{|di_1/dv_2|} \tag{2.1}$$

The bias resistance will instead be determined by

$$R_{bias} = \frac{2}{|di_2/dv_2|} \tag{2.2}$$

The data taken in the measurements will be plotted as test current against the neighbor voltage. In the plotted graphs v/i is the coefficient of slope and the 2 in second formula comes from the fact that two neighbor strips are used. The interstrip resistance is calculated for all the different bias voltages in order to find if the interstrip resistance has a dependency of the bias voltage.

2.2 C_{int} Measurement

For the interstrip capacitance measurements the AC-pads are used, this time with six probes, see fig. 2.2 . Once again one uses the concept of one test strip and the two closest neighbors. If one wants to measure the total interstrip capacitance all neighbor strips should be used as comparisons to the test strip. Since this would be very complicated setup this six probes setup are a good enough approximation.

The probes from test and neighbor strips are connected to the LCR Meter, the test strip via low voltage and the neighbors via high voltage. Outside of both the neighbor strips one more probe is touched down. Those probes are connected to ground and will work as a shield from the outer laying strips. Since the capacitance is dependent on the frequency of the AC signal, the LCR Meter will measure the interstrip capacitance for four different frequencies; 10 kHz, 100 kHz, 1 MHz and 2 MHz. The test is done at different bias voltage from 0 to -800 volts in steps of -50 volts. All the capacitance measurements were done at room temperature with nitrogen gas flowing over the detector.

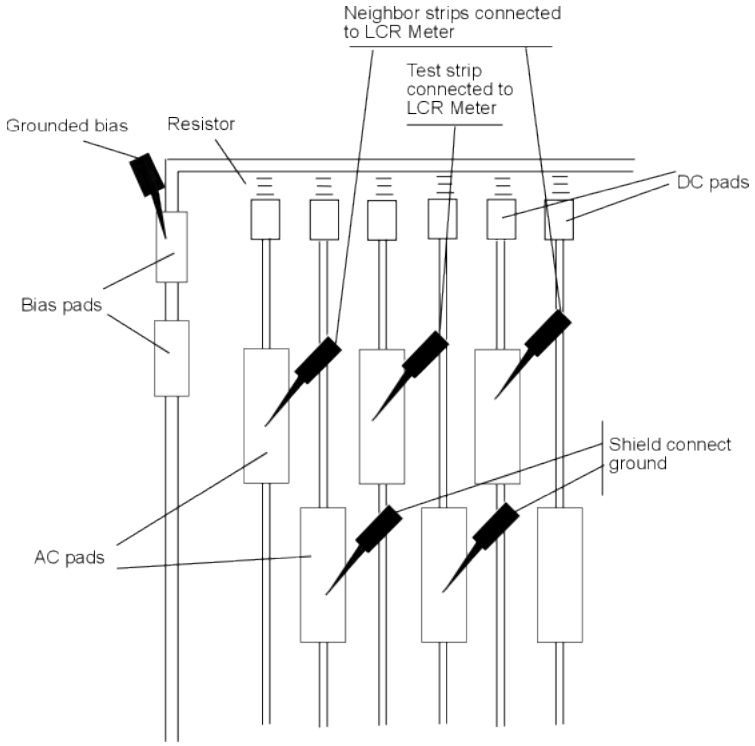

Figure 2.2: *The concept used for testing the interstrip capacitance. Probes are touched down on the AC pads of the neighbors- and test stip. A probe is also put at a bias pad and two outside the neighbor strips for shielding. The shielding probes and the bias are connected to ground while the reaming probes are connected to a LCR Meter with which help the measurement was done.*

2.3 IV Measurements

For the IV measurements only one probe is used, attached to the bias ring. The bias ring is held to ground while the backplane is tied to a high voltage which is varied between 0 and -1000 volts in steps of -50. IV curves are not taken on all detectors, just those with good interstrip characteristics to see if the structures which provide high radiation hardness would jeopardize the breakdown properties. All IV measurements were done at room temperature.

3

Results

3.1 Specific Detectors

The analysis compares pre- and post-radiated data in terms of possible effects from the different structures of the SSDs. I have chosen to not show the results for each detector since they are too many and within some categories they have similar behavior. But to give the reader an idea about the data which the comparisons are based on I am going to incorporate graphs from three individual detectors which can be representative for most detectors. I will not include any interstrip capacitance data for individual detectors since this is visible in the comparison between detectors later in the thesis.

From the collected data some different behaviors for the 2^{nd} and 3^{rd} series have been observed. The most wanted behavior is shown in fig. 3.1 with equal spacing between the different lines, i.e. the different applied bias voltage.

One can also see that there is only a slight difference in the slope coefficient between the voltages so the resistance is rather independent of the bias voltage, as seen in fig. 3.2. One can see that the resistance will first decrease with higher applied voltage but then saturate and be almost independent of the bias voltage, which is the favorable behavior.

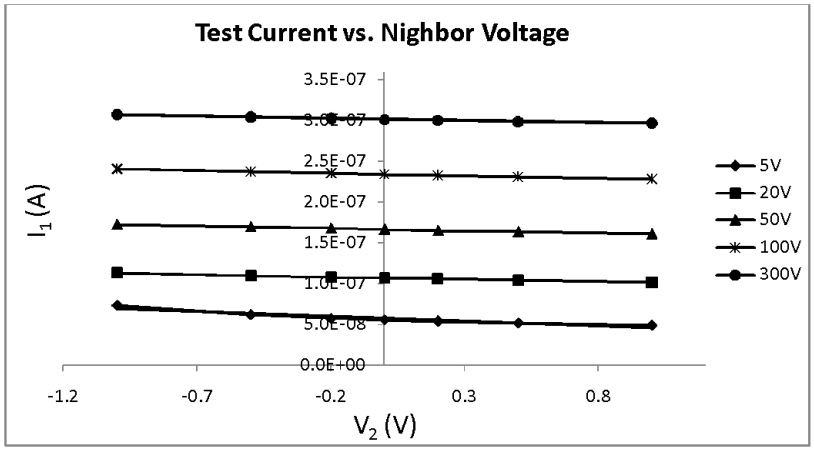

Figure 3.1: *The graph show the current in the test strip against the neighbor voltage, this for all different applied bias voltages, for detector W31-BZ5-P11 after irradiation. All data points ends up nicely on lines so the fitted trend lines agrees good with all points. For this detector the slope coefficients are similar for all applied bias voltage and the spacing between the different voltages, i.e. the lines, are rather consistent which is the wanted behavior.*

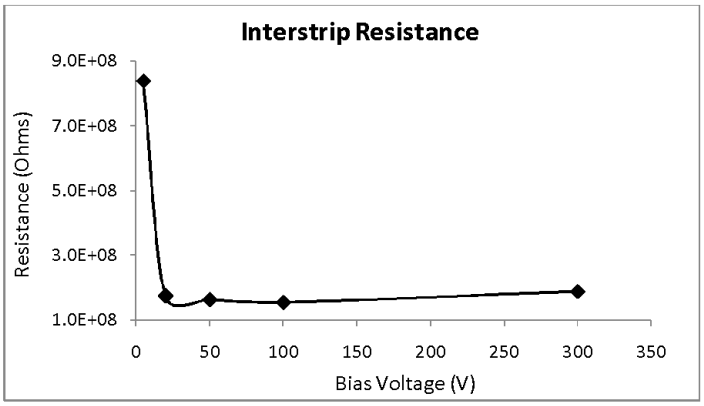

Figure 3.2: *The interstrip resistance for detector W31-BZ5-P11. The resistance is rather independent of the bias voltage which can be seen though it saturates after an applied bias voltage of about 50 volts.*

Another way to see if the resistance is high enough and if the connections of the probes have been good is to plot the current in the neighbor strip against the neighbor voltage, seen in fig. 3.3. The wanted behavior is that all lines should have the same slope coefficient and optimal be identical. From this slopes one can calculate the bias resistance as given by formula 2.2.

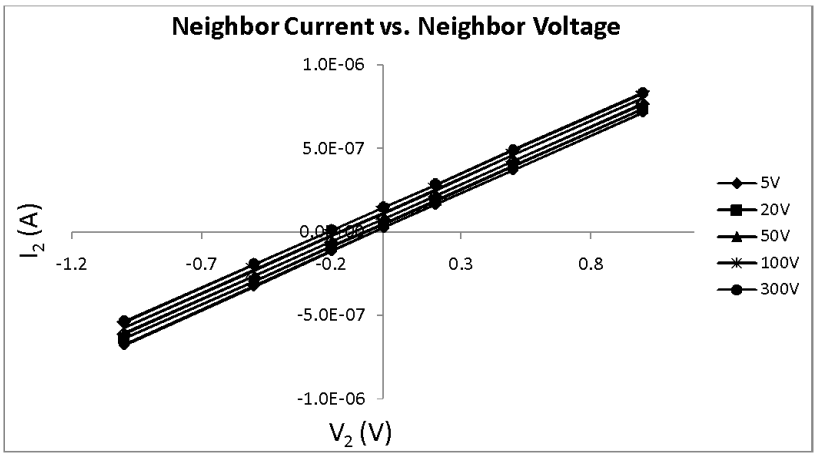

Figure 3.3: *The graph show the current in the neighbor strips against the neighbor voltage, for all applied bias voltages, for detector W31-BZ5-P11 after irradiation. The lines have rather the same slope coefficients which imply that the detector have high enough interstrip resistance, about* $5 \cdot 10^7$ *ohms and the bias resitance was calculated to about* $1.46 \cdot 10^6$ *ohms*

A slightly different behavior, but still expected, can be seen in fig. 3.4. The detector has high enough interstrip resistance. The different is that the data line does not have equal spacing, i.e. there will be slighlt different interstrip resistance depending on the bias voltage. This behavior will decrease the value for the resistance slightly and also affect the error. For detectors with data as shown in fig. 3.1 the error will be around one percent while for the detectors with data as shown in fig. 3.4 the error will be somewhat bigger, but still below 5 percent.

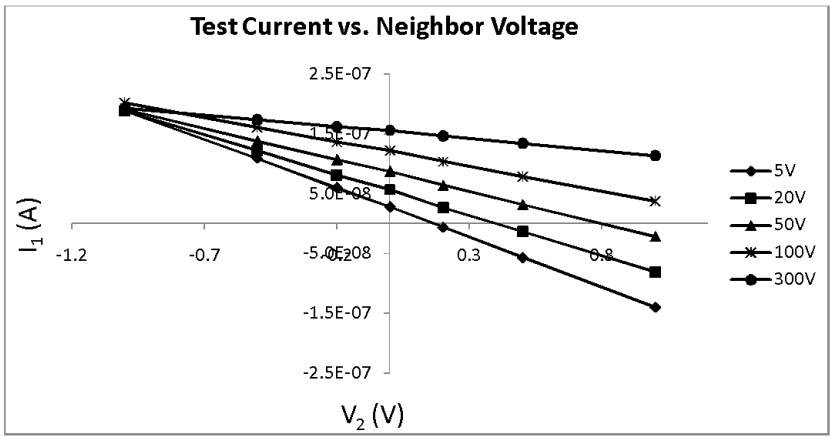

Figure 3.4: *The graph show the current in the test strip against the neighbor voltage, this for all different applied bias voltages, for detector W35-BZ5-P11 after irradiation. The lines do not have equal spacing, but all points still lies on lines which makes the fitting of the trend lines good.*

Since the interstrip resistance is calculated from the slope coefficient the different behavior will affect the interstrip resistance, as seen in fig. 3.5 Here the data show a dependency on the bias voltage, but the difference from the lowest to the highest value is not big; $1.2 \cdot 10^7$ for 5 volts to $5 \cdot 10^7$ for 300 volts.

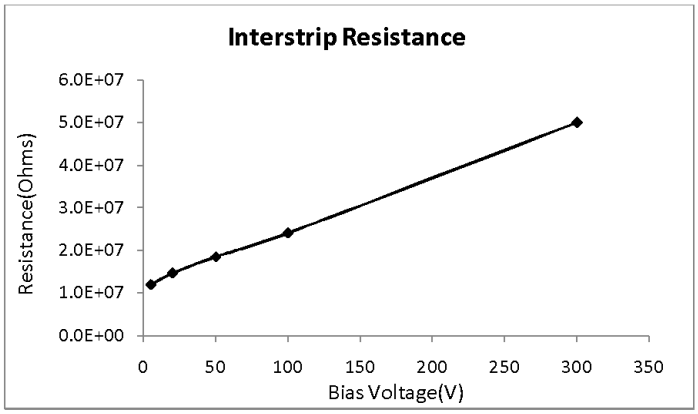

Figure 3.5: *The interstrip resistance for detector W35-BZ5-P11 after irradiation. It shows a slight increased and dependency with the bias voltage. Here the bias resistance will vary slighty from* $1.22 - 1.44 \cdot 10^6$ *ohms*

In the 3^{rd} series many detectors have a too low interstrip resistance. This can be seen in two ways; calculated values of the resistance, see fig.3.8, and from the behavior in fig. 3.6 and 3.7. If the detector has a too low interstrip resistance, values below 10^7 ohms, the lines will have the crossing behavior as in the figure 3.6-3.7. For many of those detectors also a so called turn-on voltage can be observed, meaning that the detector will have a higher resistance for higher applied bias voltages, i.e. the detector need a certain amount of applied voltage to have a high resistance. The turn-on behavior can be in the graph where the slope decreases with increasing bias voltage.

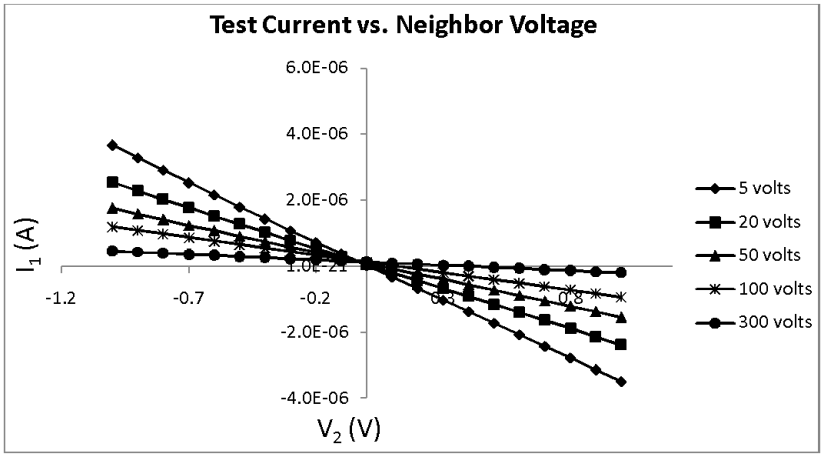

Figure 3.6: *The graph show the current in the test strip against the neighbor voltage, this for all different applied bias voltages, for detector W12-BZ4A-P4 after irradiation. This detector does not have a high enough resistance which will show from the cross-over behavior and the large values for the slope coefficients. The detector also show a turn-on behavior there higher applied voltages results in decreased slopes.*

The lack of high enough resistance can also be seen in a plot of the neighbor current against the neighbor voltage, fig. 3.7 The wanted behavior is that all lines are collected together, but for detector with too low resistance one can clearly see a division. This comes from that $V/R_{int} >> i_{leakage}$.

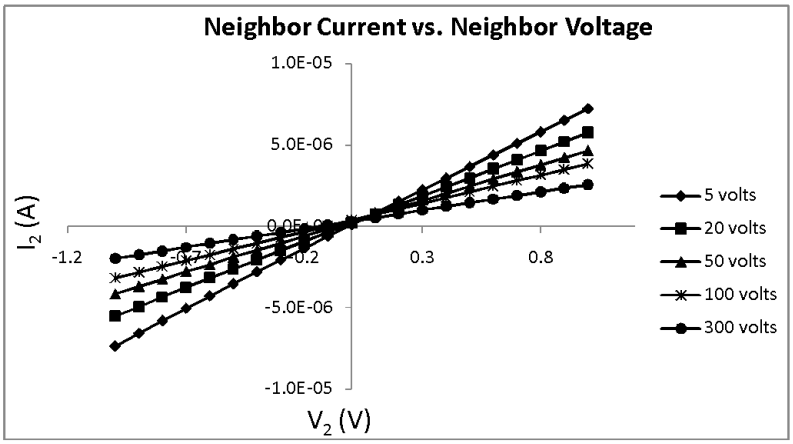

Figure 3.7: *The graph show the current in the neighbor strip against the neighbor voltage, this for all different applied bias voltages, for detector W12-BZ4A-P4 after irradiation. This detector does not have a high enough resistance which can be because the lines are not collected together as an affect of the leakage between the strips. This will also be visible in the values for the bias resistance which varies from* $3 - 9 \cdot 10^5$ *ohms*

In the graph for the calculated resistance it can see that the resistance is too low since it never exceeds 10^7 ohms. The turn-on behavior can be seen since the resistance increases almost by a factor of 10 between 5 and 300 volts.

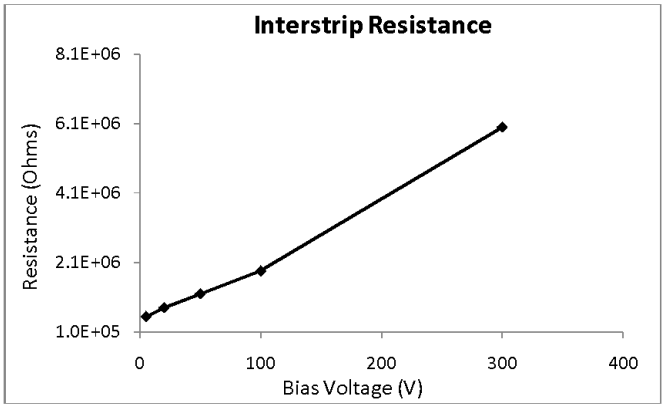

Figure 3.8: *The interstrip resistance for detector W12-BZ4A-P4 after irradiation. The resistance is clearly increasing and depended on the bias voltage. The values for the resistance never exceeds* 10^7 *ohms which imply that the detector have a too low resistance after irradiation.*

3.2 Interstrip Resistance; Comparison between all sensors

The interstrip resistance was measured for all detectors in the 2^{nd} and 3^{rd} series. The graph with all data from the 2^{nd} and 3^{rd} series can be seen in the Appendix.
For both the 2^{nd} and 3^{rd} series the pre-rad data has about the same resistance. However for the post-rad data there is a difference. For the 2nd series all lines for post-rad detectors lies within one rather collective group while for the 3rd series the data is divided into several groups with different resistance. Most of those detectors lie in groups at $4 \cdot 10^5$-$2.5 \cdot 10^7$ ohms or $2 \cdot 10^8$-$2 \cdot 10^9$ ohms. The detectors in the group with the higher resistance are shown together with the all detectors from the 2^{nd} series in fig. 3.9

3.2.1 High performance detectors

On average both series detectors have an interstrip resistance of 10^{11}-10^{12} ohms before irradiation. After irradiation they all show a clear behavior of decreasing their resistance, but for the detectors shown in fig. 3.9 their post-rad resistance is sufficiently high, i.e. they have an interstrip resistance over 10^8 ohms.

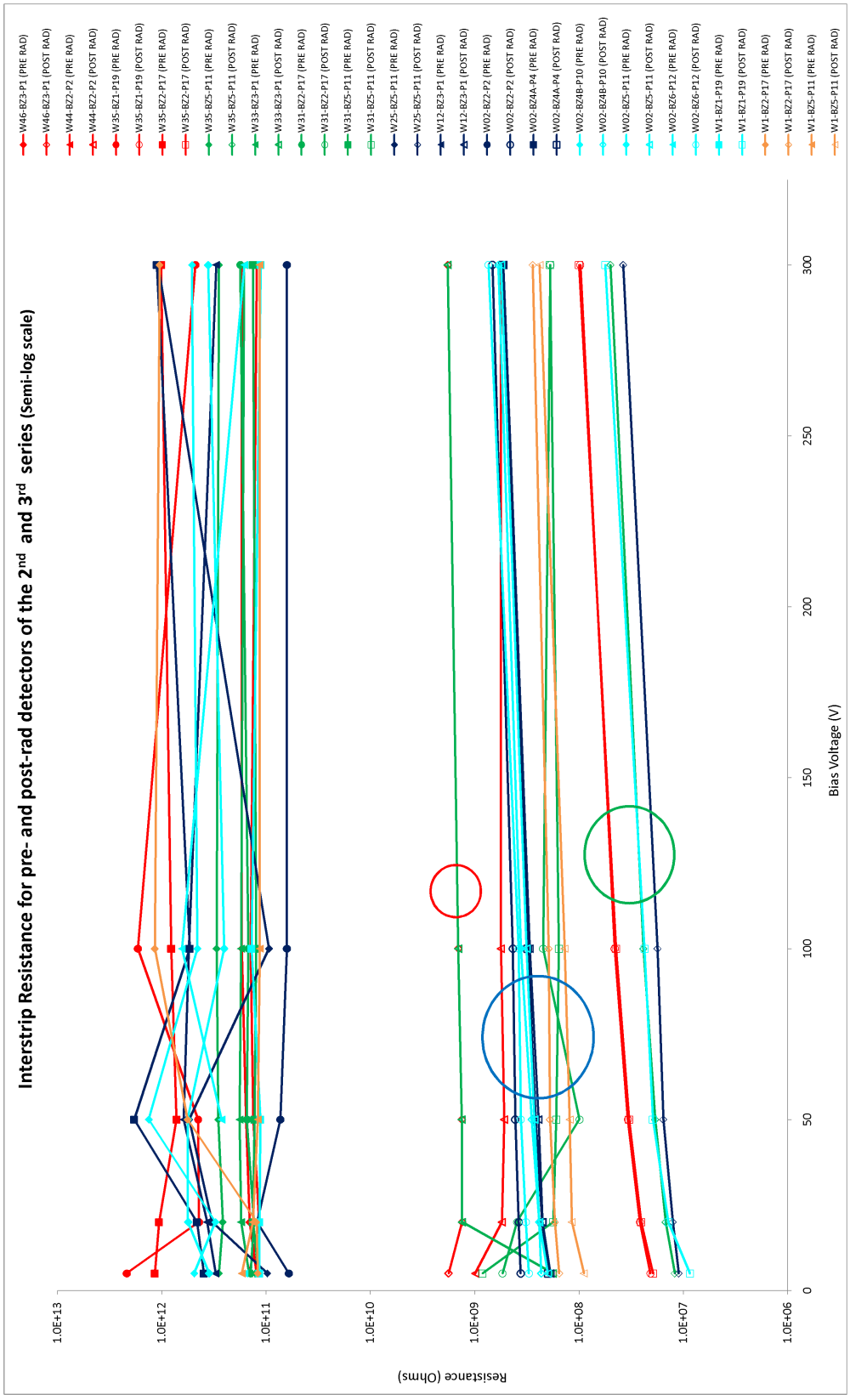

Figure 3.9: *Interstrip resistance measurements for both the pre- and irradiated detectors. The pre-rad data is shown as filled points and the post-rad as empty. The data is collected from the 2nd and 3rd series of the ATLAS upgrade program. Detector with wafer 1, 25, 31 and 35 is part of the 2nd series and the remaining is part of the 3rd series. The data which this graph is based on has a maximum error of only a few percents. The detectors with the highest resistance, red circle, have a dose of* $4 \cdot 10^{12}$ *cm*$^{-2}$ *or above. The blue circle contains detectors with a dose of* $4 \cdot 10^{12}$ *cm*$^{-2}$ *while the green circle contains detectors with a dose of* $2 \cdot 10^{12}$ *cm*$^{-2}$*. Important to remember is that the doses for detectors within the 2nd series, i.e. wafer 1, 25, 31 and 35, the doses in not exactly.*

Post-rad detectors are the most interesting. One can see that the detectors are approximately organized in terms of the total dose of p-spray and p-stops, i.e. the one with the highest dose have the higher resistance. One can also distinguish three groups, marked with three circles, see figure 3.9. Detector W46-BZ3-P1 and W33-BZ3-P1 have the highest resistance, red circle, where W46-BZ3-P1 has the highest dose, $10 \cdot 10^{12}\ cm^{-2}$, of all detectors. Detector W33-BZ3-P1 has the same dose as the detectors found in the middle group, blue circle, which has a dose of $4 \cdot 10^{12}\ cm^{-2}$. It can be seen that the two detectors with only p-spray or p-stops, W33-BZ3-P1 and W44-BZ2-P2, have a slightly higher resistance than detector with a combination of both, all wafer 02. From this it seems that there is somewhat preferable with only p-stops or p-spray rather than a combination of them both.

The final group contains detectors which lie below 10^8 ohms, green circle, which is not preferable for the full-sized SSDs. The detectors in this group have all wafer 25 or 35, except detector W1-BZ1-P19. But since this detector have zone 1, i.e. its p-stop mask is removed, all detectors indicated by the green circle have a dose of $2 \cdot 10^{12}\ cm^{-2}$. This indicates that in order to have a higher interstrip resistance than 10^8 ohms after irradiation detectors need to have a total dose of p-impurities greater or equal to $4 \cdot 10^{12}\ cm^{-2}$. However can some difference be seen between detectors with the same dose, but from different series. For detectors with a dose of $4 \cdot 10^{12}\ cm^{-2}$, the ones belonging to the 2^{nd} series have a lower resistance than the one from the 3^{rd} series. Since the difference is small they probably come from the fact that the doses for the 2^{nd} series are not exactly.

3.2.2 Low performance detectors

In the 3rd series there are many detectors which after irradiation have a too low resistance to be used for full-sized detectors, i.e. they have a resistance below 10^8 ohms. Further, many of of those detectors do not even have a high enough resistance for the shorter strips, i.e. resistance below 10^7 ohms. Figure 3.10 show all post-rad detectors from the 3^{rd} series. Detectors that have a lower resistance than 10^7 ohms all have wafers 40 or 12, except detector W02-BZ3-P1. This will be more discussed in the next sections. Those detectors have doses of p-impurities at $1 \cdot 10^{12}$ cm^{-2} which indicate that doses this low do not prevent enough of the surface damages from irradiation and they will lose too much of their interstrip resistance after irradiation. There is a slight difference between those two wafers. Detectors with wafer 40 have a somewhat higher resistance than detectors with wafer 12. All those detectors have the same dose but detectors with wafer 40 have p-spray while wafer 12 has p-stops. This indicates that p-spray is slightly favorable, for at least lower doses.

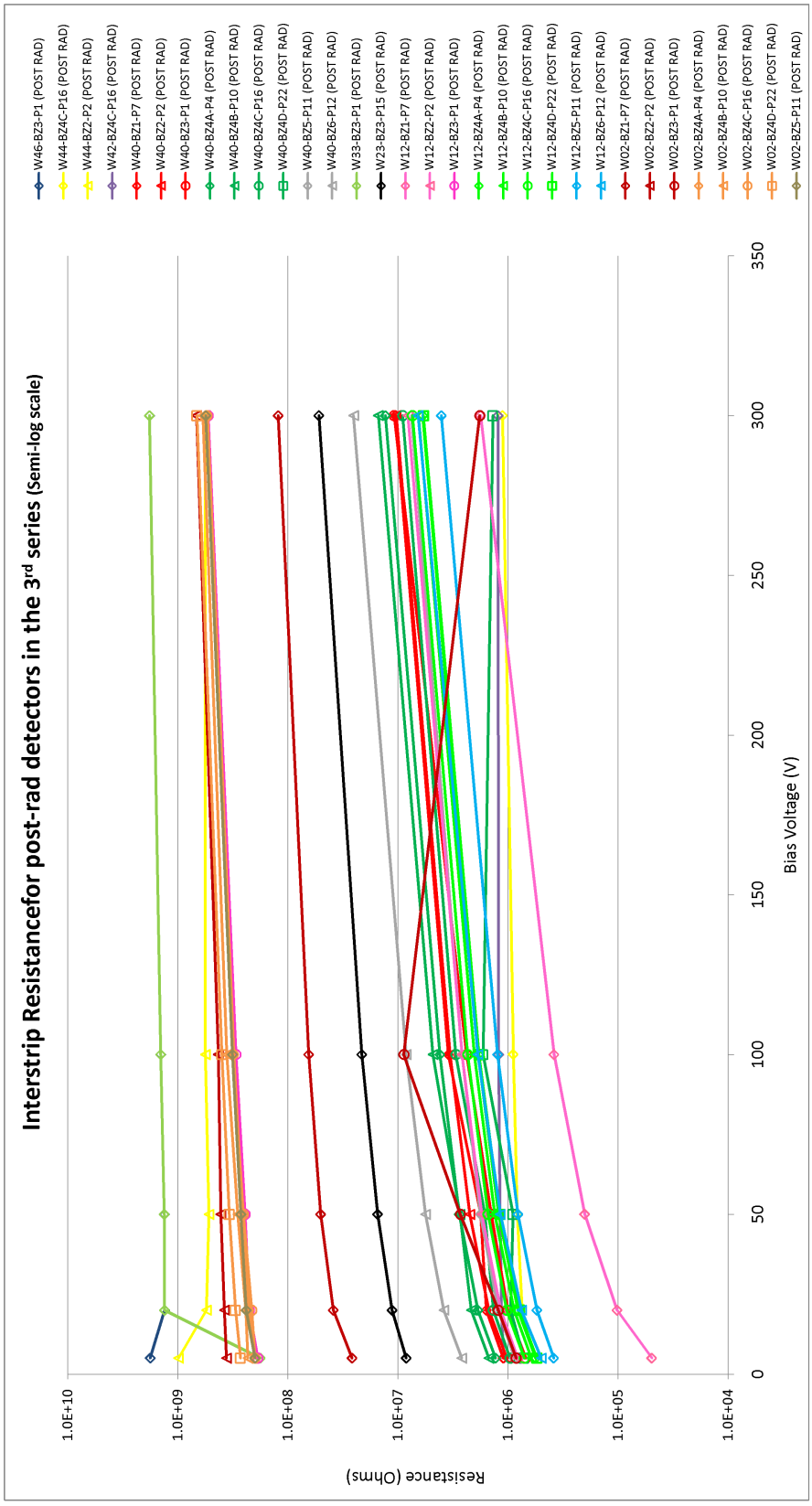

Figure 3.10: *Data from all irradiated detector of the 3rd series. The data lines are divided into different groups depending on their total dose of p-impurities in form of p-stops or p-spray. The detectors which have over 10^8 ohms all have a dose of $4 \cdot 10^{12}$ cm^{-2}. The two detectors which lie between 10^7-10^8 ohms have a dose of $2 \cdot 10^{12}$ cm^{-2} while the detectors below 10^7 ohms have $1 \cdot 10^{12}$ cm^{-2}. The detector which has an absolute lowest resistance after irradiation is the detector with either p-stop or p-spray.*

3.2.3 Zone 4; Punch-Through Protection

For the 3^{rd} series four differences version of zone 4 were produced, 4-A through 4-D. There are 3 wafer types which have zone 4, namely wafer 02, 12 and 40. The data can be divided into two groups, as seen in figure 3.11. The detectors with wafer 02 have substantial higher resistance than the remaining. The clear difference in resistance can be explained by the applied doses of p-impurities. Wafer 02 has p-stops and p-spray both to a dose of $2 \cdot 10^{12}$ cm^{-2}, total dose of $4 \cdot 10^{12}$ cm^{-2}, while wafer 12 and 40 both have a dose of $1 \cdot 10^{12}$ cm^{-2}. In the graph one can more clearly see that wafers 40 have slightly higher resistance than wafer 12 discussed in the previous section. However for the four identifications A through D, i.e. the different punch-through protection, there is no correlation between any of the four versions and a higher or lower resistance.

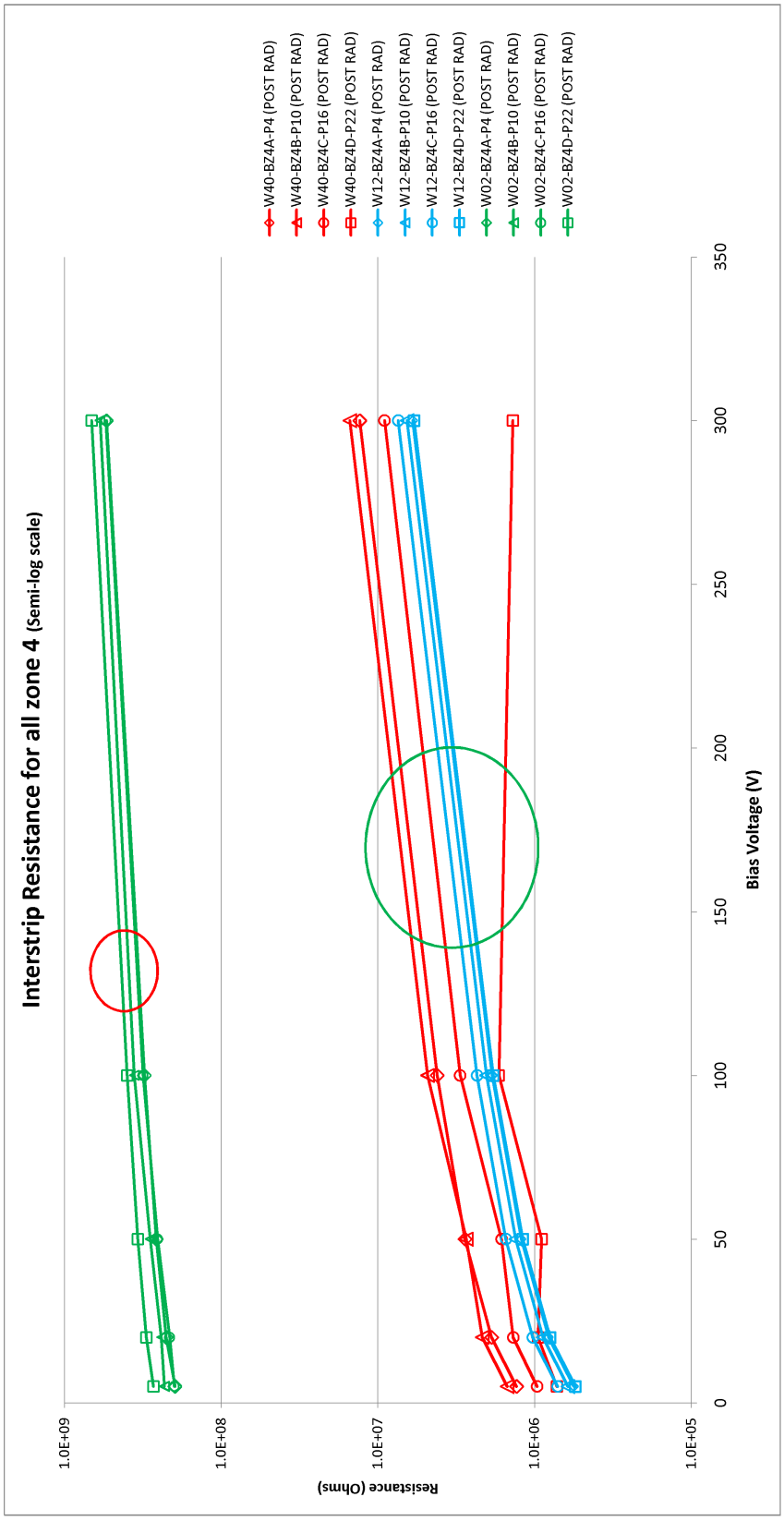

Figure 3.11: *Post-rad interstrip data for all detectors with zone 4 in the 3rd series. The graph is both color and symbol coded. In the color coding detectors with wafer 02 are green, wafer 12 blue and wafer 40 red. Regarding the different punch-through protection, i.e. identification A, B, C and D, all detectors with A have diamonds markers, B triangles, C circles and D as squares. As can be seen there is a clear separation due to the different interstrip resistance which depends on the dose of p-spray and p-stops. Wafer 02 has a total dose of $4 \cdot 10^{12}$ cm^{-2}, while wafer 12 and 40 has doses of $1 \cdot 10^{12}$ cm^{-2}. But for different punch-through protection one cannot see any correlation.*

3.2.4 Effective Dose

One can see in the previous figures that the resistance after irradiation is crucially dependent on the dose of p-spray and p-stops. Therefore detectors with the most well understood zones, zone 2 and 3, are plotted in one graph with the pre- and post-rad data, see figure 3.12. Only detectors from the 3^{rd} series have been chosen since those doses are exactly given by the manufactory. However, detector W02-BZ3-P1 and W12-BZ3-P1 have been excluded due to their odd behavior, discussed in more detail in section 3.6.

In the figure it can be seen that all pre-rad data is lying collected in one group around 10^{11} ohms. The post-rad data can be divided into three groups depending on their resistance. The ones with the highest, indicated by a red circle, have only decreased their resistance with about 10^2 ohms after irradiation. And they all lie above the needed 108 ohms which is needed for development of full-sized detectors. All detectors in this category have a total dose of p-impurities of $4 \cdot 10^{12}\ cm^{-2}$ or above. The detector with lies below this group, indicated with a green circle, have a total dose of $2 \cdot 10^{12}\ cm^{-2}$. This detector have a lower resistance than the required for full-sized detectors, but still above 10^7 ohms which is the minimum resistance for the mini-SSDs of the pre-series. The last group contains detectors which have too low resistance to be properly functional, indicated by a blue circle. The total dose for all those detectors is $2 \cdot 10^{12}\ cm^{-2}$. From this graph one can once again see the importance of a minimum dose of $4 \cdot 10^{12}\ cm^{-2}$ then constructing future SSDs, especially with longer strips.

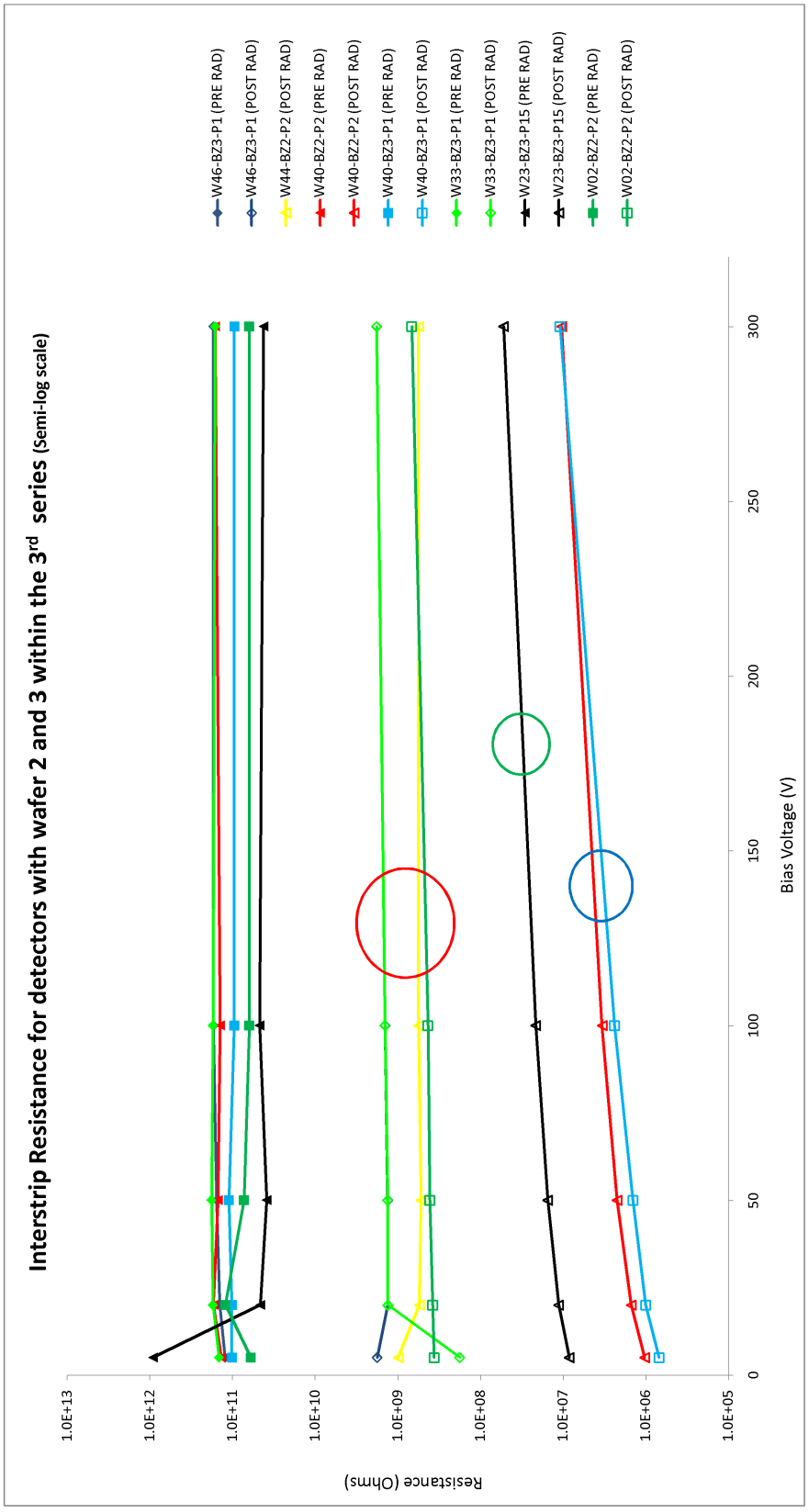

Figure 3.12: *Show detectors with wafer 2 and 3 from the 3rd series, both pre- and post-rad data. Here one can see that detectors with the highest resistance after irradiation all have doses above $4 \cdot 10^{12}$ cm^{-2}, red circle. The one indicated by the green circle have a dose of $2 \cdot 10^{12}$ cm^{-2} and finally the one which the lowest resistance, blue circle, have only a dose of $1 \cdot 10^{12}$ cm^{-2}. This shows clearly that to have a resistance above 10^8 ohms after irradiation one needs doses of p-spray or p-stops of at least $4 \cdot 10^{12}$ cm^{-2}.*

3.3 Interstrip Capacitance; Comparison between all sensors

3.3.1 Second Series

The 2^{nd} series show no common behavior in the interstrip capacitance which will predict what will happen to all detectors after irradiation. Two of them show an increase in their capacitance after irradiation, and for six of them it is decreased, as seen in figure 3.13. Also within this division there is no clear correlation between a specific structure and if the capacitance will increase or decrease after irradiation.

For the detectors with decreased capacitance we found all wafer 1 and 31; wafer 1 has a combination of p-spray and p-stop to a total dose of $4 \cdot 10^{12}$ cm^{-2} and wafer 31 only p-stops to a dose of $4 \cdot 10^{12}$ cm^{-2}. However out of the detectors with wafer 1, one have a dose of only $2 \cdot 10^{12}$ cm^{-2} since it has zone 1 and the last detector with decreased capacitance have wafer 35, p-stops to a dose of $2 \cdot 10^{12}$ cm^{-2}, so no correlation based on the dose can be seen. Regarding the zones, we find two detectors with zone 1, two with zone 2 and two with zone 5. So neither here any correlation can be seen.

Detectors which have an increase in their capacitance all have wafer >20, i.e. either only p-spray or p-stops; wafer 35 have p-spray to a dose of $2 \cdot 10^{12}$ cm^{-2} and wafer 25 have p-stops to a dose of $2 \cdot 10^{12}$ cm^{-2}. They both has zone 5, i.e. narrow metal. So within this group the detectors seem to have common structures. However do the detectors which have an decrease in their capacitance share many of the same properties so neither here can any conclusions be made.

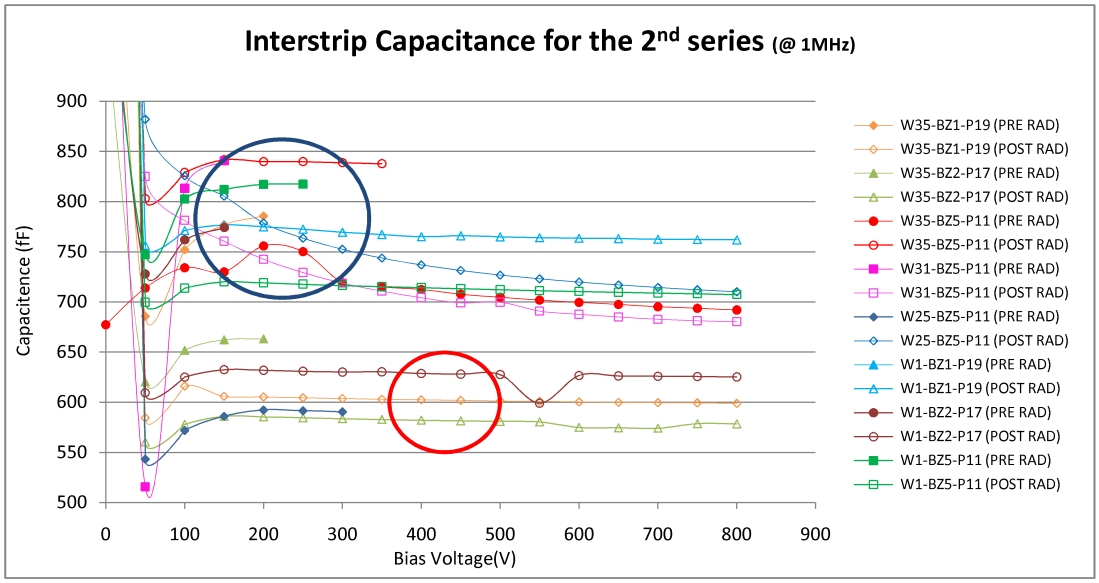

Figure 3.13: *The interstrip capacitance for all detectors in the 2^{nd} series. Data for the both the pre and irradiated detectors are taken at a frequency of 1MHz. The pre-rad data for detector W1-BZ5-P11 and W1-BZ1-P19 is equal so the data point for the second one of those is hidden behind the first. One can see that for post-rad detectors, detectors with zone 5 in average have a higher capacitance than detectors with zone 2.*

Even if there are no similarities between the changes of capacitance one can see some similarities between the different zones and the actual values, especially for post-rad detectors. Almost all detectors with a higher capacitance have zone 5, narrow metal, indicated by a blue circle while the detectors with a lower capacitance have instead zone 2 or 1, indicated by a red circle. Specific for detectors with zone 2 are that they have individual p-stops, i.e. each strip is surrounded. Detectors with zone 1 have instead their p-stop mask is removed. Regarding the total dose one cannot see any correlations. The three detectors with the highest capacitance have doses of $2 \cdot 10^{12}$ cm^{-2}, the three middle ones have doses of $4 \cdot 10^{12}$ cm^{-2} and finally the three with the lowest capacitance have a dose of $2 \cdot 10^{12}$ cm^{-2}. However, it is important to remember that those doses are not exactly given by the manufactory which might cause errors in the analysis.

The detectors with increased capacitance, detector W35-BZ5-P11 and W25-BZ5-P11, have a slightly different behavior. The capacitance for these detectors and W31-BZ5-P11 never fully saturates which differs from the remaining detectors behavior which first decrease, followed by a slight increase to finally saturation.

3.3.2 Third series

The collected data from the capacitance measurements for the 3^{rd} series have been divided into two graphs; one with the all detectors with zones 3, both pre- and post-rad data and one with the remaining tested detectors.

A difference from the 2^{nd} series is that all pre-rad detectors with zone 3 in the 3^{rd} series have similar interstrip capacitance, around 650fF, see figure 3.14. Another difference is that one can divided the irradiated detectors into two groups depending on their behavior. For three detectors the capacitance will first rapidly decrease, increase a little and finally saturate at values around 650fF, so about the same value as before irradiation. However, if one looks closely all capacitance values are increase after irradiation, especially for detectors W46-BZ3-P1.

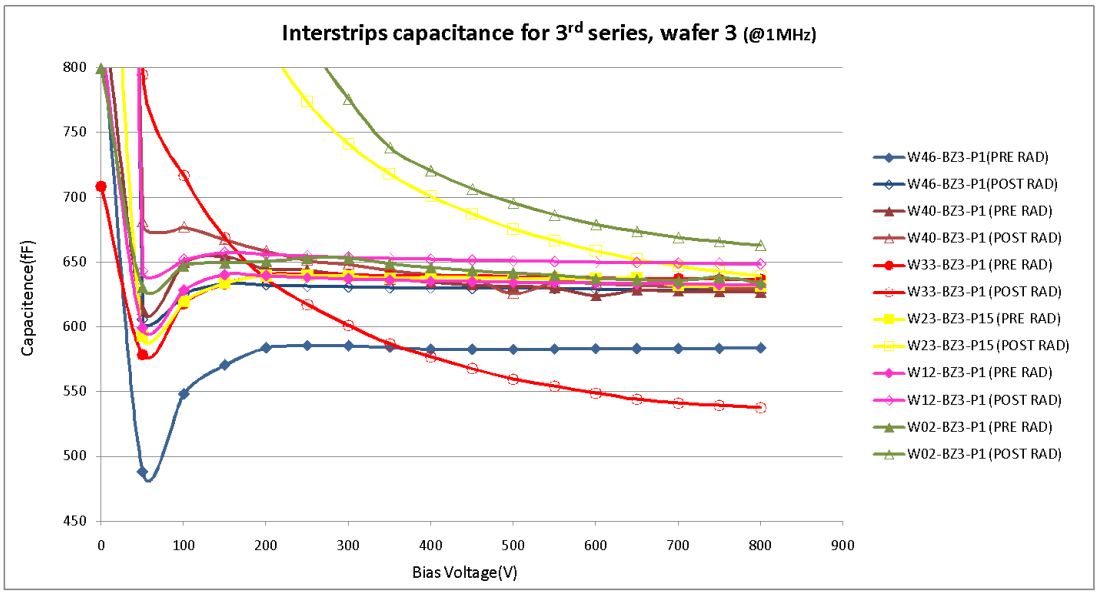

Figure 3.14: *The interstrip capacitance for the detectors within the 3^{rd} series with zones 3. There are two different behaviors for the irradiated detectors, three of them have a clear saturation behavior while for the remaining three their capacitance is decreasing throughout the whole range of taken measurements.*

Detector W02-BZ3-P1, W23-BZ3-P15 and W33-BZ3-P1 have another behavior after irradiation, their capacitance will decrease rather steady throughout the whole region of taken data and it does not show any indications of saturation. This is similar behavior to what was seen for some of the detectors in the 2^{nd} series, but it is more extreme for the detectors in the 3^{rd} series. Since there is no sign of saturation and the decrease is so big, it is harder to determine if the capacitance decrease or increase after irradiation. For detector W33-BZ3-P1 is probably decreased since all post-rad data points after -200 volts lie below the pre-rad. Also the possible saturation for the other two detectors will most likely lie below the pre-rad data. However, for all values before -800 volts the post-rad data lies above. This will affect the scatter plots since the capacitance values used is the once at -300 volts.

For two of the detectors with different behavior, W02-BZ3-P1 and W33-BZ3-P1, this probably can be explained by damage on their surface. Photos of the damages can be seen in the Appendix. Those damages have probably arisen due to a high charge collection on the surface then operating the detector. The problematic is that no such damage was found on for detectors W23-BZ3-P15 which can explain why it behaves similar to the damage detectors.

The data shown in figure 3.15 is pre-rad data from detectors with wafers 02 and 44, but more importantly those detectors have zone 1, 2 and 4. Overall the detectors seem to have a slightly different behavior, less saturating, than the other detectors seen in figure 3.13 and 3.14. The probably biggest reason for this is the difference in scale for the graphs.

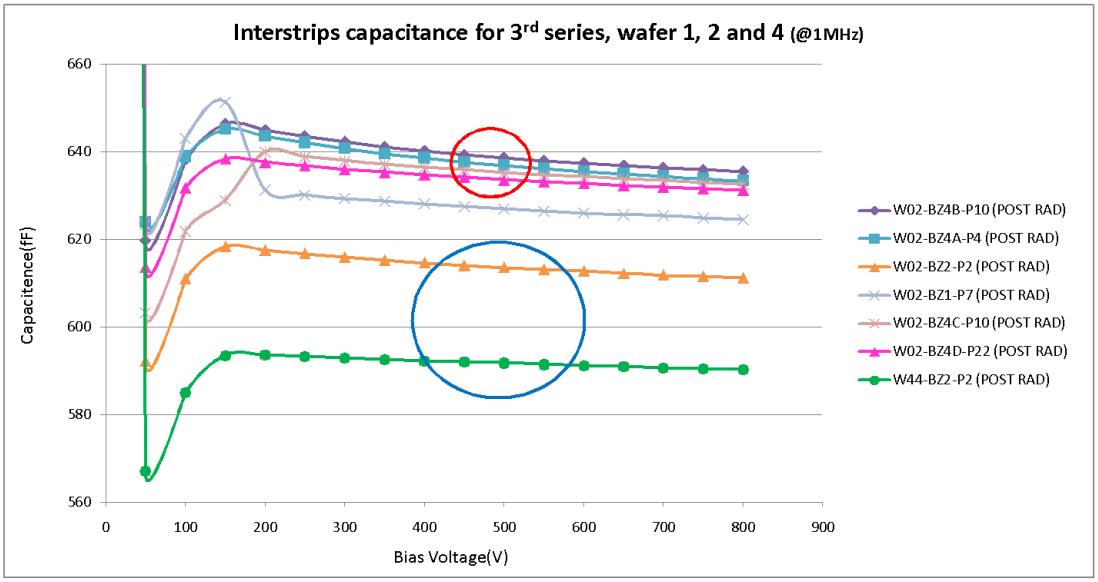

Figure 3.15: *The interstrip capacitance for the detectors within the 3^{rd} series which have high interstrip resistance. It can be seen that zone 2 have the lowest capacitance, zone 4 the highest and zone 1 lies in the middle.*

For this data one cannot really make any comparisons between the dose of p-impurities and the capacitance since all detectors, except W02-BZ2-P7, have the same dose. Regarding the zones it can be seen that all detectors with zone 4 has similar values and have the highest capacitance, indicated by a red circle. The detector with zone 1 has a slightly lower capacitance and the two detectors with zone 2 have substantially lower capacitance, indicated by a blue circle. These results are consistence with the results from the 2nd series, seen in figure 3.13, there the detectors with zone 2 have among the lowest capacitance and also zone 1 show rather low capacitance.

3.4 Resistance vs. Capacitance

To compare the interstrip resistance and capacitance at the same time a scatter plots with the resistance against the capacitance is made, as seen in the following figures. Detectors which have the wanted interstrip properties will lie in the upper left corner in these graphs.

3.4.1 Second series

In the data from the 2nd series one can see that the resistance decrease after irradiation for all detectors and as earlier found there is no common behavior for all detectors regarding their capacitance after irradiation which makes some of the data points move to the left and some to the right.

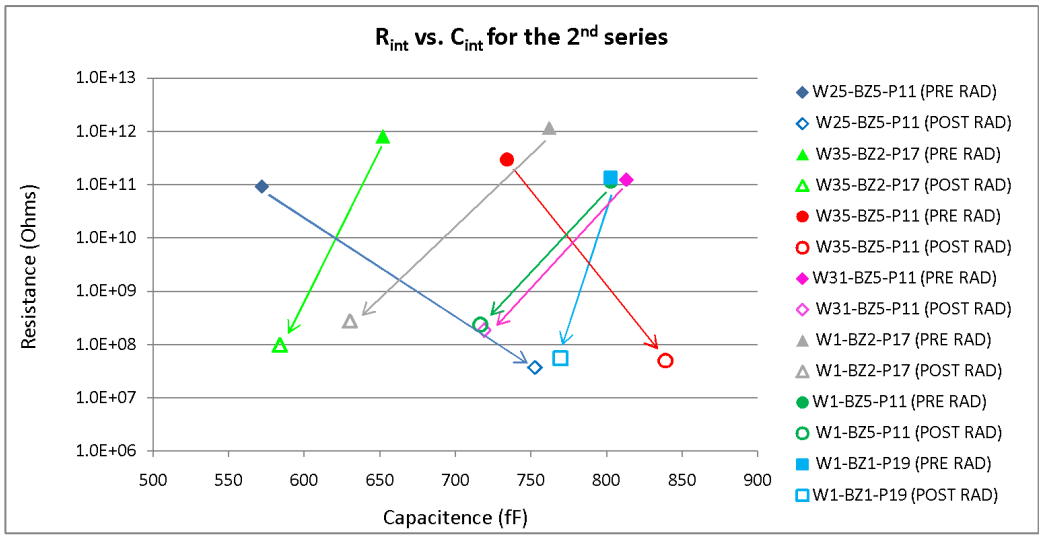

Figure 3.16: *The resistance data plotted against the capacitance data for each detector in the 2^{nd} series. The pre-rad data is shown as filled points and the post-rad as empty points. The data for each point, both for interstrip resistance and capacitance is taken at same bias voltage which for pre-rad data is 100 volts and post-rad is 300 volts. All the capacitance values are taken at 1MHz. One can see that all detectors have a decrease in their resistance, and most of them also a decrease in the capacitance. The detectors with the most wanted behavior are W35-BZ2-P1 and W1-BZ2-P2.*

As can be seen in figure 3.16, detector W35-BZ2-P17 has the most preferable behavior in the 2^{nd} series. Before irradiation it is located within the area in the upper left corner and after irradiation it still in the left part of the diagram. Detector W1-BZ2-P17 also shows a likable behavior, even if it does not lie within the wanted area before irradiation. It is similar to detector W35-BZ2-P17, in that they both show a lowering of their capacitance after irradiation, as indicated by the green and grey arrow.

On the other side of the scale we have detector W25-BZ5-P11 and W35-BZ5-P11 which both show bad behavior in both interstrip capacitance and resistance after irradiation, as indicated by the purple and red arrow.

Here again it can be seen the fact that it seems like detectors with zone 5 have a higher capacitance than the detectors with the remaining zones. However there is no indication that detectors with zone 5 will have an increased capacitance after irradiation. This is the case for the two above mention detectors, but detector W1-BZ5-P11 and W31-BZ5-P11 have a lower capacitance after irradiation, indicated by the dark green and pink arrow.

3.4.2 Third series

It is harder to compare the data for the 3^{rd} series in a scatter plot since detectors W02-BZ3-P1, W23-BZ3-P15 and W33-BZ3-P1 never saturate which make the data points chosen based upon the saturation points for the other detectors. This is probably partially the reason for the big increase of capacitance for detector W23-BZ3-P15 and W02-BZ3-P1, indicated by a red and a dark green arrow. As one could see in figure 3.14 the capacitance values for those detectors is rather far from the pre-rad value at 300 volts but will become closer when higher bias voltage applied.

For detectors with zone 3 in the 3^{rd} series it can be seen that they, except the two above mention detectors, have rather low capacitance after irradiation. The biggest problem for those detectors is instead the resistance. The decrease for some detector is so big so the scale had to be plotted in log scale and they do not depending as exactly as the remaining zones on the dose of p-impurities.

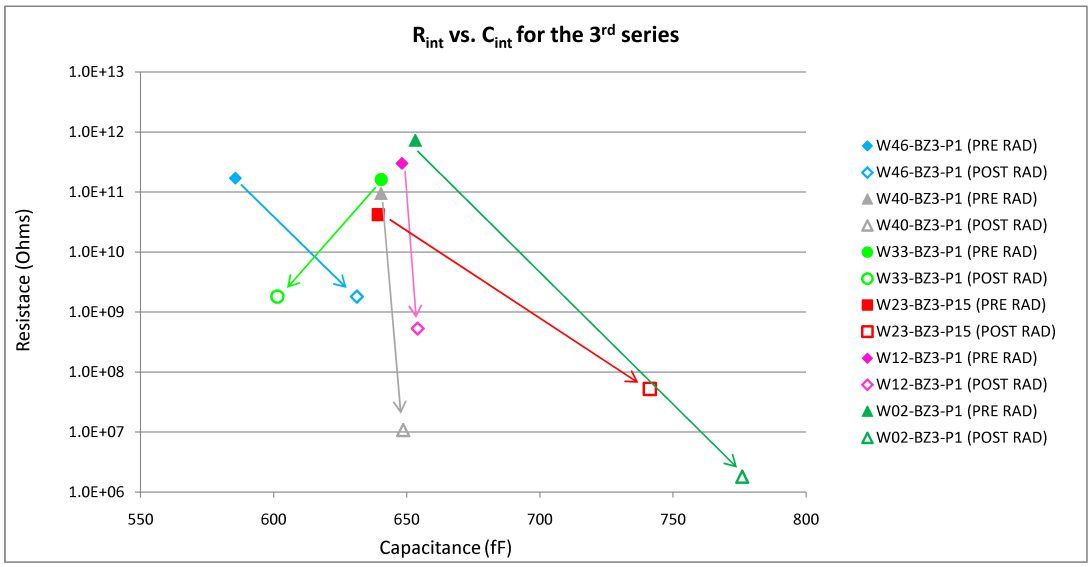

Figure 3.17: *The capacitance data plotted against the resistance data for each detector in the 3nd series. The data for each point, both for interstrip resistance and capacitance is taken at same bias voltage which for both are 300 volts. All the capacitance values are those at 1MHz. Detector W46-BZ3-P1 and W33-BZ3-P1 have the most preferable behavior.*

As an example all detectors with wafer 02, except the one with zone 3, have among the highest resistance of all detectors while detector W02-BZ3-P1, dose $4 \cdot 10^{12}\ cm^{-2}$, have lower resistance than detector W12-BZ3-P1 and W40-BZ3-P1 which both have doses of p-impurities, $1 \cdot 10^{12}\ cm^{-2}$. Another example is detector W12-BZ3-P1 which has almost the same resistance as detectors with much higher doses like detector W46-BZ3-P1, a dose of $10 \cdot 10^{12}\ cm^{-2}$.

Figure 3.19 show a scatter plot with the post-rad data for the tested detectors within the 2^{nd} and 3^{rd} series. Two interesting difference can be seen between the different series. The dominating amount of the detectors with highest resistance is from the 3^{rd} series, indicated by a green circle.

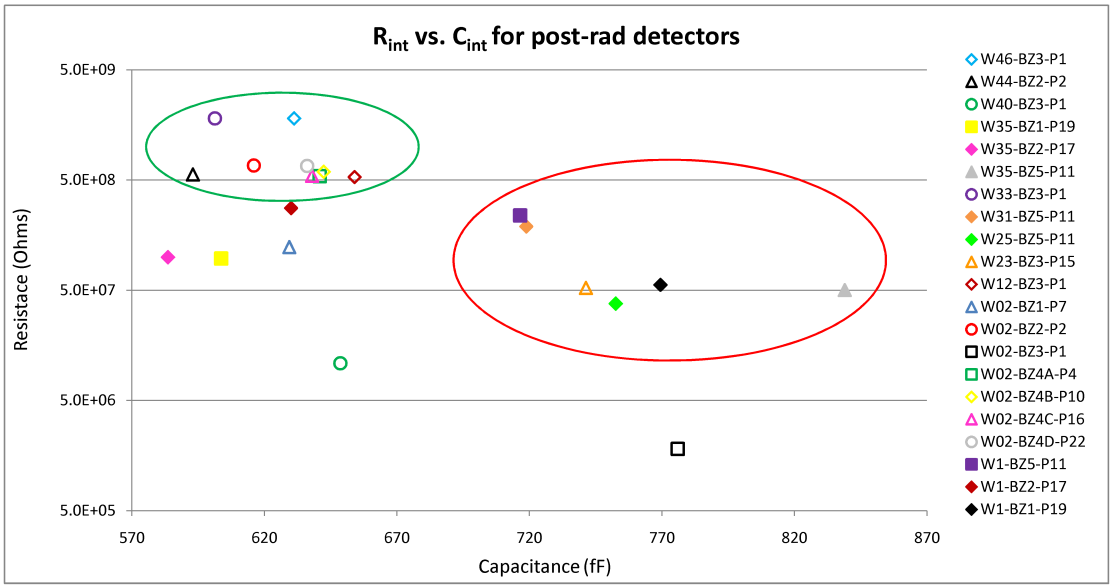

Figure 3.18: *The scatter plot between the resistance and capacitance. Data is taken for tested detector after irradiation. Data points from the 2^{nd} series are shown as filled points and from the 3^{rd} series as empty points.*

This depends on that most of those detectors have higher doses of p-impurities. Another interesting observation is that all detectors with high capacitance values than 700fF, except W23-BZ3-P15 and W02-BZ3-P1, are part of the 2^{nd} series, indicated by the red circle. This is probably due to the fact that most of those detectors have zone 5 which seems unfavorable for a low capacitance.

3.5 Odd behaving detectors

As seen in the analysis there is some detectors which do not follow the expected behavior. Regarding the interstrip resistance there is primary two detectors which do not give the same values as detectors with the same wafer, which is expected. The first detector is W12-BZ3-P1 which has a much higher resistance than the remaining detectors with wafer 12. The second one is detector W02-BZ3-P1 which instead has a lower resistance than the remaining with detectors of wafer 02. From their breakdown voltage one cannot find an explanation since neither of them breaks down within the operation voltage. However have surface damage has been found on detector W02-BZ3-P1 which might explain this, see the Appendix, but no such damage have been seen on detector W12-BZ3-P1.

Regarding the interstrip capacitance there is two different forms of behavior which is questionable. The first is the behavior discussed around figure 3.14. Detector W02-BZ3-P1, W23-BZ3-P15 and W33-BZ3-P1 have another behavior after irradiation than the normal, i.e. their capacitance decrease rather steady for all data points and show no indications of saturation. For detector W02-BZ3-P1 and W33-BZ3-P1 this can probably be explained from the observed damage on the surface, see the Appendix, while detector W23-BZ3-P15 have no visible damage or early breakdown.

The second group of detectors that do not follow the expected behavior contains detector W02-BZ3-P1, W23-BZ3-P15 and W1-BZ1-P19. Those detectors have a higher capacitance than detectors with the same zone. For detector W02-BZ3-P1 and W23-BZ3-P15 this might be partially explained from the fact that they do not saturate within the taken data region. This means that the data points used in the scatter plots are based upon the saturation point for the other detectors and if one would taken the data from a higher voltage they should have lower capacitance values. But detector W1-BZ1-P19 has saturated for the point used in the scatter plot and it does not break down within the tested region.

3.6 Breakdown voltage

IV measurements were performed after irradiation for two reasons; determine if good interstrip properties come with the disadvantage of a low breakdown voltage and to see if there the detectors which have an odd behavior would break down within operation voltage.

One can see that all the detectors in the 3^{rd} series have a high breakdown voltage, most of them do not break down in the region for which the test was preformed, i.e. down to -1000 volts, as seen in figure 3.20. Detectors, detector W12-BZ3-P11, W23-BZ3-P15 and W33-BZ3-P1 show a slight trend of breakdown around -900 volts. Out of those detectors W33-BZ3-P1 have favorable interstrip properties and all of them have a strange behavior compared to the expected, discussed in the section 3.6.

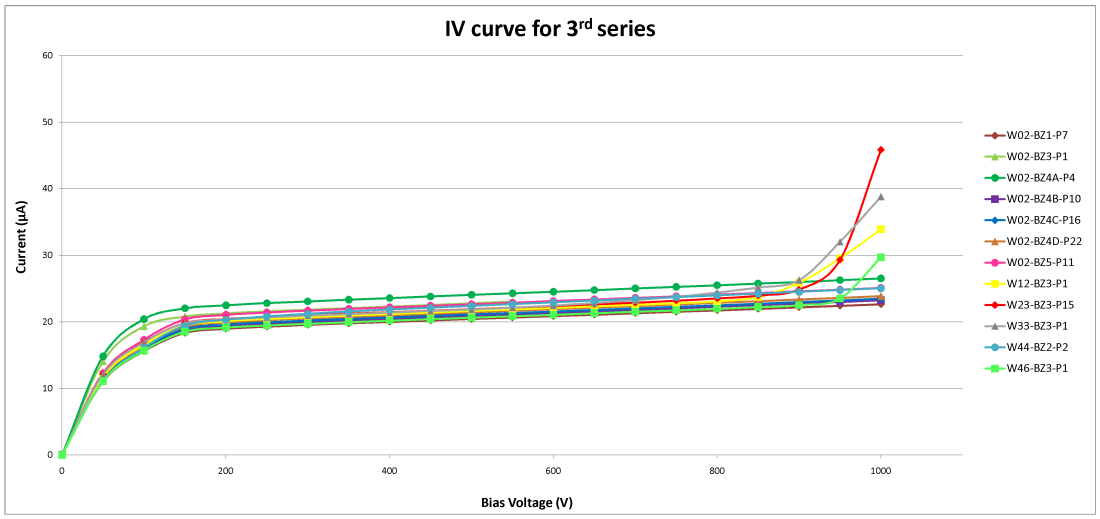

Figure 3.19: *The break down behavior for the detectors in the 3^{rd} series after irradiation. The data is taken between 0 and -1000 volts. The data shows that all detectors, except W12-BZ3-P11, W23-BZ3-P15 and W33-BZ3-P1, do not break done within the tested region. But also detectors which break down do so at a high applied voltage, around -900 volts.*

However with this high breakdown voltage, it has probably no affect the resistance and capacitance measurements. The breakdown also lie above the promised by manufactory that the detectors should function to at least -600 volts.

Detectors from the 2^{nd} series have a slightly lower breakdown voltage compared to the 3^{rd} series, as seen in figure 3.21. Four detectors will break down within the tested region; detector W31-BZ2-P17, W25-BZ5-P11, W35-BZ1-P19 and W35-BZ2-P17.All of them break down around -800 volts. Out of those we find the three with the highest resistance and also both of the zone 2:s, which have the best overall interstrip properties. However, also those breakdowns are probably too high to affect the interstrip measurements and they all are above the -600 volts.

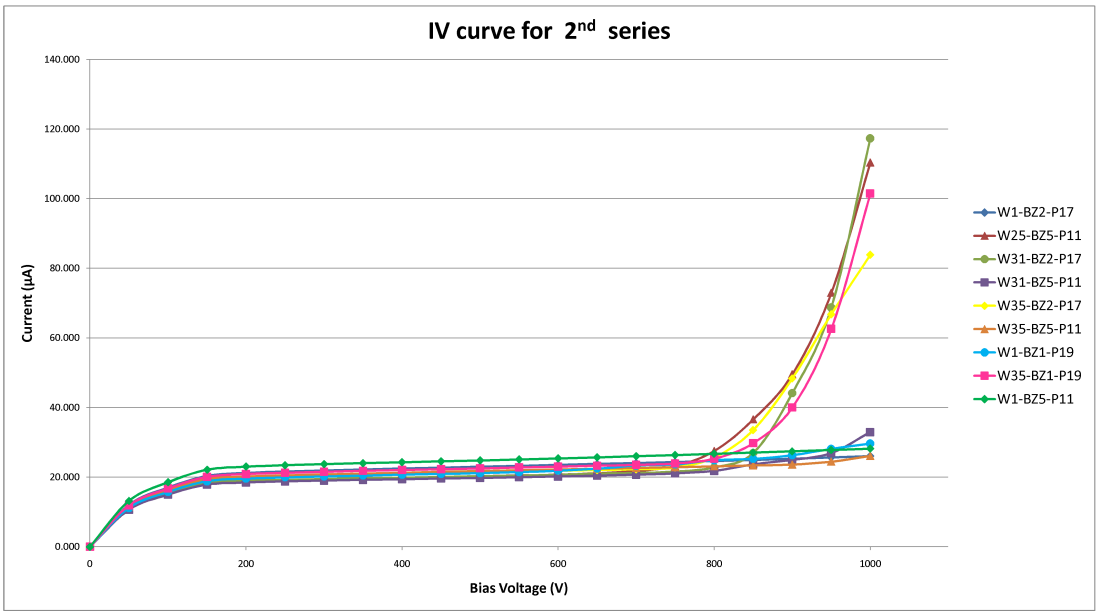

Figure 3.20: *The breakdown voltage for the 2^{nd} series. The data is taken between 0 and -1000 volts. One can see that four detectors are breaking down around 800 volts while the remaining does not show any behavior of breakdown within the tested range.*

4

Conclusions

Comparing the detectors with the same wafer from the 2^{nd} and 3^{rd} series it can be seen that they agree well for most difference zones, with the biggest differences are found within zone 3:s. The interstrip resistance mostly will depend on the wafer of the detectors, i.e. the total dose of p-spray or p-stops. The correlation between the 2^{nd} and 3^{rd} series is also good, except some slight differences which probably depends on the fact that the doses for the 2^{nd} series are not exact. In the post-rad data from both series the detectors are approximately organized in terms of the total dose of p-spray and p-stops, i.e. the one with the highest dose have the higher interstrip resistance. The detectors which have a dose of $2 \cdot 10^{12}$ cm^{-2} have a high enough resistance for the mini-SSDs with 1 cm long strips. However to provide resistance enough for the full-size detector for ATLAS the resistance need to be over 10^8 ohms which is only provided for detectors with a total dose of $4 \cdot 10^{12}$ cm^{-2} or higher. From the data it is also clear that detector with a dose of only $1 \cdot 10^{12}$ cm^{-2} after irradiation does not have a high enough interstrip resistance.

The data for capacitance for the 2^{nd} and 3^{rd} series indicates that the capacitance is almost only depending on the zones. Neither of the detectors showed any correlation between the different doses of p-impurities and the capacitance, neither pre- nor post-rad. When compare the different zones it can be that zone 5 after irradiation have a capacitance around 800fF while the remaining zones have capacitance from 600fF-650fF. This shows that detectors with zone 5 are unfavorable. The detectors which have the lowest interstrip capacitance are detectors with zone 2 and therefore seem to be the most favorable, while detectors with zone 1, 3 and 4 have a slightly higher capacitance but not more than about 50fF. However, the data within this thesis do not show that the zones will determine if the capacitance will increase or decrease after irradiation.

The future productions should be based on detectors with doses of at least $4 \cdot 10^{12}\ cm^{-2}$ if one wants to apply the dose for a full-sized detector for ATLAS in order to have a high enough interstrip resistance after irradiation. Regarding if a higher dose than the minimum of $4 \cdot 10^{12}\ cm^{-2}$ is preferable no indication neither for nor against have been observed. The detector analyzed with a higher dose has about the same resistance and capacitance after irradiation as the detectors with a dose of $4 \cdot 10^{12}\ cm^{-2}$. Regarding the preference of zones, zone 2 is slightly favorable, even if they in average do not have a significantly lower capacitance than detectors with zone 1, 3 and 4.

However, one should be a little careful with those zones. One need to take into account that zone 1 has no p-stops which will lower or remove any total dose which contain p-stops.

Regarding zone 4, the difference with the punch-through protection is not well understood and they are not made for p-spray which makes limitation and need for further investigation. Finally, detectors with zone 3 have in this thesis shown an inconsistency in their resistance compared to the expected depending on their doses. This might be an effect from that some of them were damage, maybe even more detectors was found. However, also here a further investigation is needed with more variations of zone 3. The clearest conclusion regarding zones is between zone 5 and the remaining. Compared with all remaining detectors, the ones with zone 5 have a much higher capacitance both before and after irradiation ad should therefore be avoid in any future production of SSDs.

5

Appendix

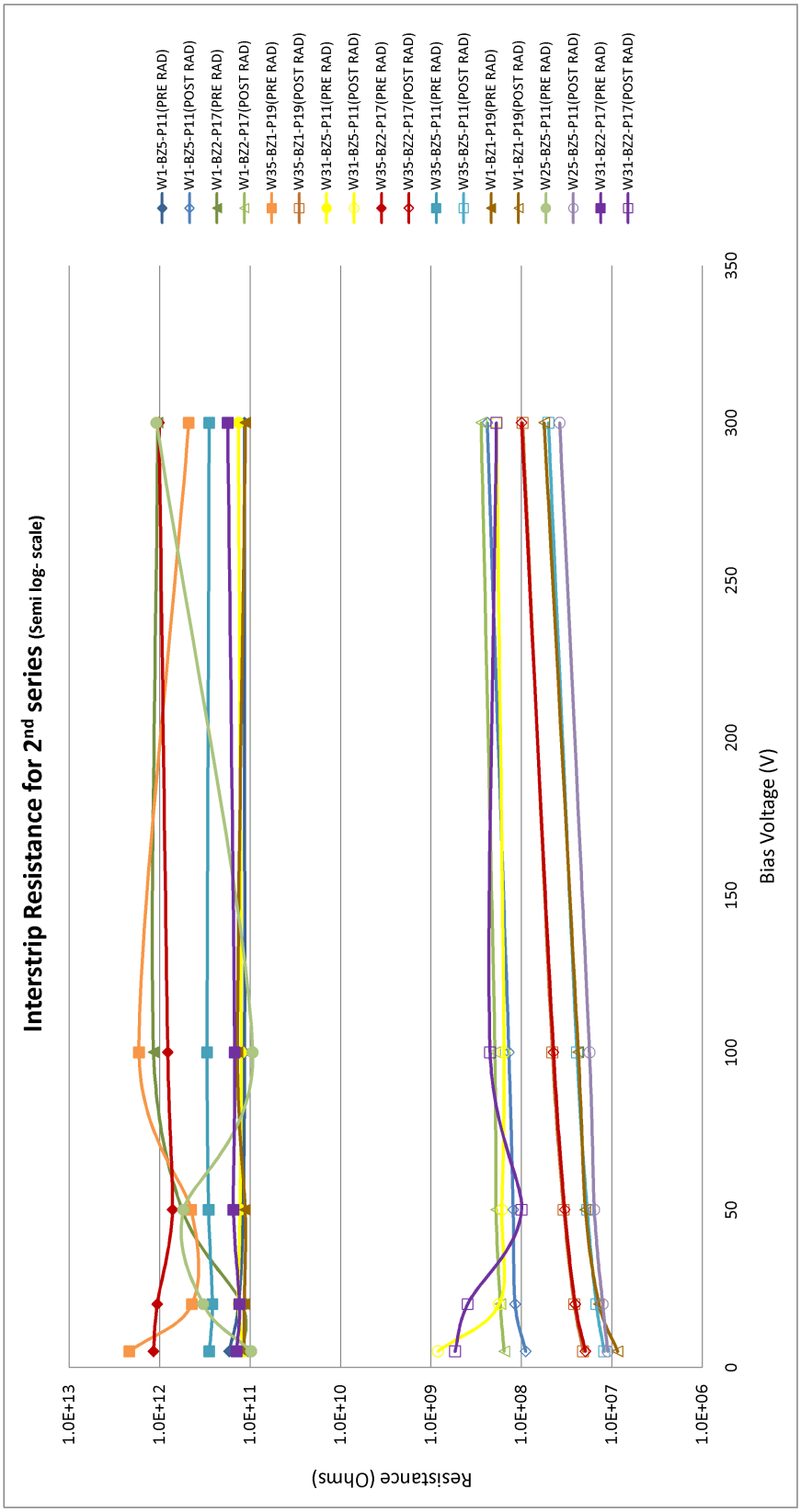

Figure 5.1: *All data from the 2nd series*

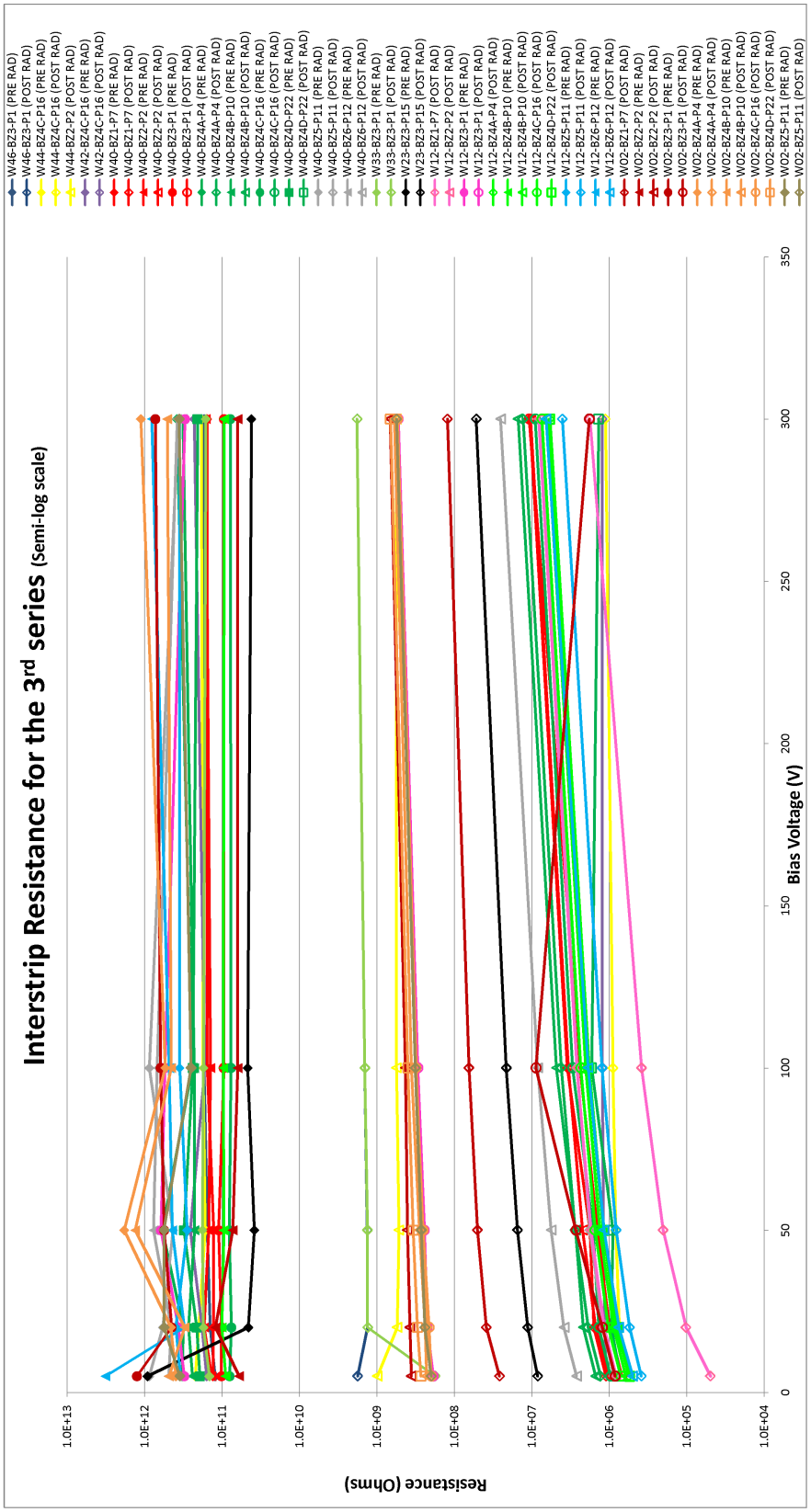

Figure 5.2: *All data from the 3rd series*

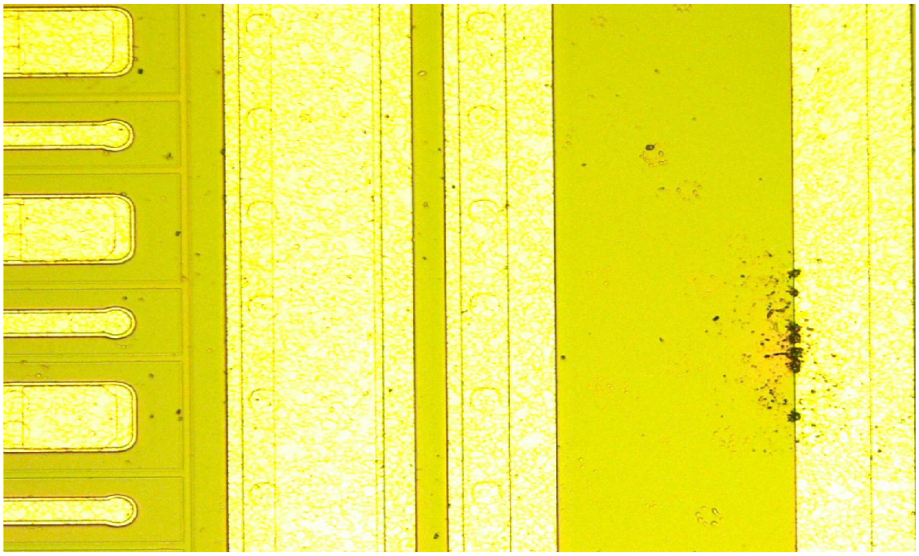

Figure 5.3: *The surface damage on detector W02-BZ3-P1*

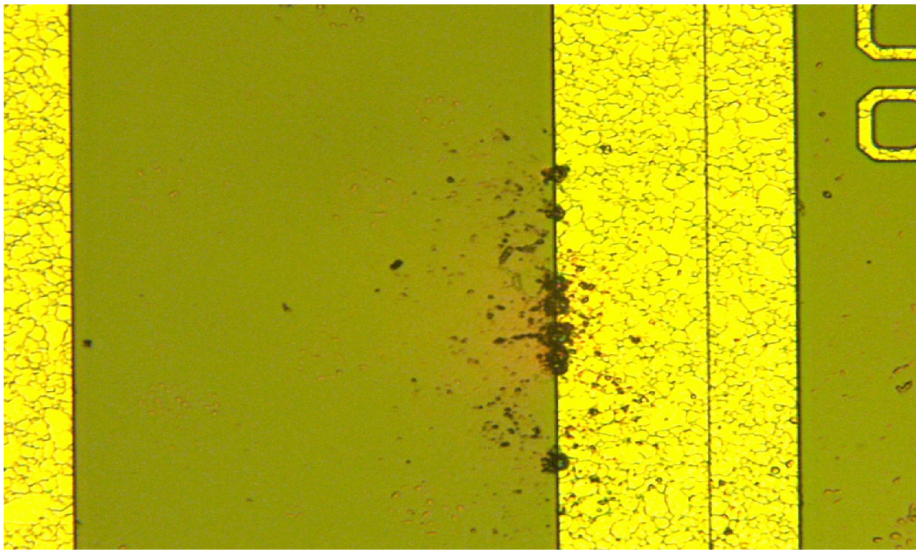

Figure 5.4: *A zoomed photo of the damage on detector W02-BZ3-P1*

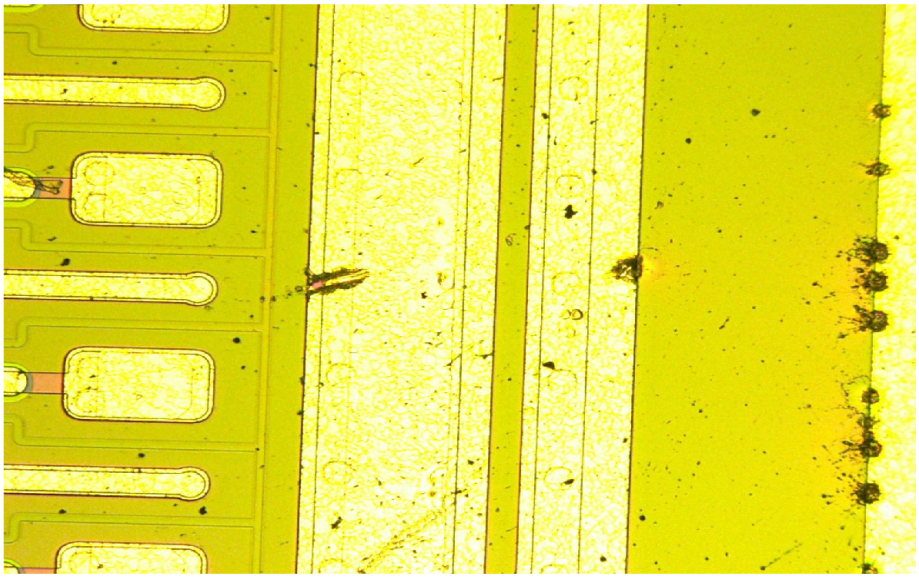

Figure 5.5: *The surface damage on detector W33-BZ3-P1*

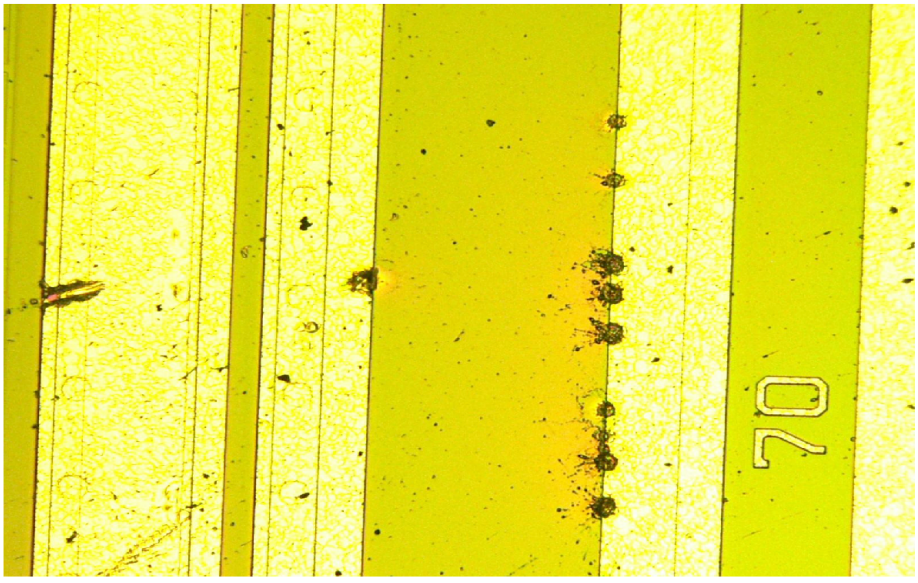

Figure 5.6: *A zoomed photo of the damage on detector W33-BZ3-P1*

Bibliography

[1] Erik H. M. Heijne, "1980, a revolution in silicon detectros, from energy spectrometer to radiation imager: Some technical and historical details", Nuclear Instruments and Methods in Physics Research A591 (2008) 6-13

[2] Ian W. Henderson, "Effects of -Irradiation on P-type Silicon Strip Detector", B.S. Thesis, University of California at Santa Cruz, Physics Dept. Santa Cruz, CA, June 2006

[3] John Wray, "Characterization of the irst prototype p-type silicon strip sensor", B.S. Thesis, University of California at Santa Cruz, Physics Dept. Santa Cruz, CA, August 2005

[4] Mara Bruzzi, Hartmut F.-W. Sadrozinski, Abraham Seiden, "Comparing radiation tolerant material and devices for ultra rad-hard tracking detectors"

[5] D. H. Kah et al. "Development and test of silicon strip detector for international linear collider", Nuclear Instruments and Methods in Physics Research A579 (2007) 745-749

[6] S. Yoshida et al. "Radiation hardening of silicon strip detectors", Nuclear Instruments and Methods in Physics Research A514 (2003) 38-43

[7] Y. Unno. "ATLAS07 Strip Program", Presentations given ATLAS upgrade Week, 2009/2/25

[8] Y. Unno, "Strip Sensor Status", Presentations given ATLAS upgrade Week NIKHEF 2008/11/04

[9] K. Yamamoto et al. "A study on the interstrip capacitance of double-sided silicon strip detectors", Nuclear Instruments and Methods in Physics Research A326 (1993) 222-227